



Mild Traumatic Brain Injury Induces Transient, Sequential Increases in Proliferation, Neuroblasts/Immature Neurons, and Cell Survival: A Time Course Study in the Male Mouse Dentate Gyrus

Lyles R. Clark^{1,2*}, Sanghee Yun^{1,2}, Nana K. Acquah^{1,3}, Priya L. Kumar^{1,4}, Hannah E. Metheny¹, Rikley C. C. Paixao¹, Akivas S. Cohen^{1,2} and Amelia J. Eisch^{1,2*}

OPEN ACCESS

Edited by:

Jose Angel Morales-Garcia,
Complutense University of Madrid,
Spain

Reviewed by:

Steven G. Kernie,
Columbia University, United States
Shaun W. Carlson,
University of Pittsburgh, United States

*Correspondence:

Lyles R. Clark
k.lyles.clark@gmail.com
Amelia J. Eisch
eisch@upenn.edu

Specialty section:

This article was submitted to
Neurodegeneration,
a section of the journal
Frontiers in Neuroscience

Received: 30 September 2020

Accepted: 02 December 2020

Published: 07 January 2021

Citation:

Clark LR, Yun S, Acquah NK, Kumar PL, Metheny HE, Paixao RCC, Cohen AS and Eisch AJ (2021) Mild Traumatic Brain Injury Induces Transient, Sequential Increases in Proliferation, Neuroblasts/Immature Neurons, and Cell Survival: A Time Course Study in the Male Mouse Dentate Gyrus. *Front. Neurosci.* 14:612749. doi: 10.3389/fnins.2020.612749

¹ Department of Anesthesiology and Critical Care Medicine, The Children's Hospital of Philadelphia (CHOP) Research Institute, Philadelphia, PA, United States, ² Mahoney Institute for Neurosciences, Perelman School of Medicine, Philadelphia, PA, United States, ³ Biological Basis of Behavior Program, University of Pennsylvania, Philadelphia, PA, United States, ⁴ Biomechanical Engineering, University of Pennsylvania, Philadelphia, PA, United States

Mild traumatic brain injuries (mTBIs) are prevalent worldwide. mTBIs can impair hippocampal-based functions such as memory and cause network hyperexcitability of the dentate gyrus (DG), a key entry point to hippocampal circuitry. One candidate for mediating mTBI-induced hippocampal cognitive and physiological dysfunction is injury-induced changes in the process of DG neurogenesis. There are conflicting results on how TBI impacts the process of DG neurogenesis; this is not surprising given that both the neurogenesis process and the post-injury period are dynamic, and that the quantification of neurogenesis varies widely in the literature. Even within the minority of TBI studies focusing specifically on mild injuries, there is disagreement about if and how mTBI changes the process of DG neurogenesis. Here we utilized a clinically relevant rodent model of mTBI (lateral fluid percussion injury, LFPI), gold-standard markers and quantification of the neurogenesis process, and three time points post-injury to generate a comprehensive picture of how mTBI affects adult hippocampal DG neurogenesis. Male C57BL/6J mice (6-8 weeks old) received either sham surgery or mTBI via LFPI. Proliferating cells, neuroblasts/immature neurons, and surviving cells were quantified via stereology in DG subregions (subgranular zone [SGZ], outer granule cell layer [oGCL], molecular layer, and hilus) at short-term (3 days post-injury, dpi), intermediate (7 dpi), and long-term (31 dpi) time points. The data show this model of mTBI induces transient, sequential increases in ipsilateral SGZ/GCL proliferating cells, neuroblasts/immature neurons, and surviving cells which is suggestive of mTBI-induced neurogenesis. In contrast to these ipsilateral hemisphere findings, measures in the contralateral hemisphere were not increased in key neurogenic DG subregions after LFPI. Our work in this mTBI model is in line with most literature on other and more severe models of TBI in showing TBI stimulates the process of DG neurogenesis. However, as

our DG data in mTBI provide temporal, subregional, and neurogenesis-stage resolution, these data are important to consider in regard to the functional importance of TBI-induced of the neurogenesis process and future work assessing the potential of replacing and/or repairing DG neurons in the brain after TBI.

Keywords: neurogenesis, TBI, dentate gyrus, proliferation, LFPI

INTRODUCTION

Traumatic brain injury (TBI) is a leading cause of death and disability in the United States, affecting ~2.8 million new people annually (Report to Congress on Mild Traumatic Brain Injury in the United States, 2003; Taylor et al., 2017). TBI is a mechanical event that results in primary focal and/or diffuse brain injury, often with secondary pathological sequelae and long-term neurological consequences (Sterr et al., 2006; Daneshvar et al., 2011; Katz et al., 2015). TBIs in humans are heterogeneous in location, severity, and mechanism, but are typically classified as mild, moderate, or severe based on severity and duration of acute symptoms (Narayan et al., 2002). Most research has focused on moderate and severe injuries due to their dramatic impact on brain health and cognition (Lippert-Grüner et al., 2006). However, the majority of brain injuries sustained are classified as mild TBIs (mTBIs) (Faul et al., 2010; Taylor et al., 2017). mTBIs induce no gross structural brain abnormalities, but can lead to lasting cognitive deficits - particularly in regard to attention and memory (Daneshvar et al., 2011; Katz et al., 2015). Injury-induced cognitive deficits in the absence of gross brain damage can be replicated in rodent models of mTBI (Lyeth et al., 1990; Eakin and Miller, 2012). Notably, many of the cognitive deficits seen in both rodents and humans after TBI involve hippocampal-dependent functions, such as spatial and contextual memory and pattern separation (Witgen et al., 2005; Smith et al., 2012; Folweiler et al., 2018; Paterno et al., 2018). These cognitive deficits are accompanied by electrophysiological changes in the hippocampus, including hyperexcitability in the dentate gyrus (DG; Folweiler et al., 2018). The DG typically acts as a “filter” or “gate,” with sparse activity limiting how much information is relayed through to downstream areas (Hsu, 2007). One theory about mTBI-induced cognitive deficits posits that this “DG gate” breaks down after injury, leading to excessive DG depolarization which spreads to area CA3 (Folweiler et al., 2018), thus disrupting this “gating” of information flow through the hippocampus and causing cognitive dysfunction. Although an excitatory/inhibitory imbalance is thought to mediate injury-induced cognitive deficits, the cellular and network mechanisms underlying these mTBI-induced physiological and cognitive deficits are unknown.

One potential contributor to rodent mTBI-induced physiological changes and cognitive deficits is mTBI-induced changes in the generation of new hippocampal DG granule cells. This process of DG neurogenesis consists of “stages,” including proliferation (cell division of stem cells and their progeny in the subgranular zone [SGZ]), generation of neuroblasts and immature neurons, and cell survival of mature, glutamatergic DG

granule cells (Aimone et al., 2014; Bond et al., 2015; Kempermann et al., 2015). The bidirectional relationship between the activity of the DG as a whole and the process of neurogenesis has been well-studied (Ma et al., 2009; Ikrar et al., 2013; Kempermann, 2015; Temprana et al., 2015). While the exact function of adult-born DG granule cells is under debate, they are implicated in hippocampal-based cognition such as contextual memory and pattern separation (Clelland et al., 2009; Tronel et al., 2010; Sahay et al., 2011; Nakashiba et al., 2012). The process of DG neurogenesis also contributes to circuit excitability in both physiological (Ikrar et al., 2013) and pathological conditions like epilepsy (Cho et al., 2015; Neuberger et al., 2017). Given that the process of neurogenesis has potent influence over hippocampal physiology and function, there is great interest in understanding how it - and associated hippocampal physiology and function - is changed after brain injury.

Indeed, many preclinical studies suggest the process of adult hippocampal DG neurogenesis is changed after TBI (Aertker et al., 2016; Ngwenya and Danzer, 2018; Bielefeld et al., 2019). However, the direction of the change is disputed. TBI is reported to decrease (Gao et al., 2008; Hood et al., 2018), increase (Dash et al., 2001; Kernie et al., 2001; Blaiss et al., 2011; Villasana et al., 2015; Sun, 2016; Neuberger et al., 2017), or not change (but rather increase glial cell proliferation; Chirumamilla et al., 2002; Rola et al., 2006) the process of DG neurogenesis. These discrepancies are likely related in part to differences in experimental parameters, including time point post-TBI, “stage” of the process examined, approach to quantify the neurogenesis process, and TBI model used and its severity. To this end, it is notable that rodent models of mild brain injury - including lateral fluid percussion injury (LFPI), blast trauma, and weight drop - also produce mixed effects on the process of DG neurogenesis (Bye et al., 2011; Wang et al., 2016; Neuberger et al., 2017; Tomura et al., 2020). Given that new neuron replacement has been suggested as a potential treatment for TBI-induced cognitive dysfunction (Blaiss et al., 2011; Sun et al., 2015; Aertker et al., 2016; Sun, 2016), and the prevalence of mTBI in humans, it is surprising that only two rodent studies have examined injury-induced effects on the process of DG neurogenesis after mTBI caused by LFPI. One LFPI study in mice reported the number of neuroblasts/immature neurons labeled by doublecortin (DCX) in the ipsilateral DG increased to the same magnitude in Sham and mTBI mice vs. control mice (Aleem et al., 2020). However, this study only examined DCX-immunoreactive (+) cells 7 days post-injury (dpi), which urges study of additional time points; also this study did not provide neurogenesis quantification methods, making it unclear whether this neurogenesis result is meaningful. A very comprehensive LFPI study in rat sampled

4 time points post-injury and used stereology to quantify cells labeled with markers of several stages of the neurogenesis process, and definitely showed a transient increase in DCX+ cells 3 dpi (Neuberger et al., 2017). However, this study was performed in juvenile rats, leaving open the question of how mTBI changes the process of neurogenesis in the adult mouse. In light of the cognitive and physiological hippocampal changes seen in the mTBI mouse model (Witgen et al., 2005; Smith et al., 2012; Folweiler et al., 2018; Paterno et al., 2018), it is important to address this major knowledge gap: how does a clinically relevant model of mTBI change the dynamic process of DG neurogenesis in the adult mouse?

To fill this knowledge gap, we exposed adult male mice to LFPI or Sham and examined stages of DG neurogenesis at short-term (3 dpi), intermediate (7 dpi), and long-term (31 dpi) time points. The clinically relevant model LFPI was used because it causes two changes in mice that are also seen in humans after mTBI: (1) both focal and diffuse injury but no necrotic cavity (Smith et al., 2012; Xiong et al., 2013; Brady et al., 2018) and (2) cognitive deficits, such as worse hippocampal-based spatial memory (Folweiler et al., 2018). In our study, we collected indices of proliferation (number of Ki67+ cells at all time points, number of BrdU+ cells 3 dpi), neuroblasts/immature neurons (number of DCX+ cells at all time points), and cell survival (number of BrdU+ cells 7 and 31 dpi). We find the ipsilateral DG neurogenic regions of LFPI mice have more proliferation 3 dpi, more neuroblasts/immature neurons 7 dpi, and more new cell survival 31 dpi relative to these regions in Sham mice. These results suggest this model of mTBI produces a transient increase of DG neurogenesis in canonical DG neurogenic regions, consistent with the increased neurogenesis seen after other and more severe models of TBI. We discuss this and other interpretations of our DG data, and consider the implications for the temporal, subregional, and neurogenesis-stage resolution data provided here for the first time in a mouse model of mTBI.

METHODS

Mice

Experiments were performed on 6- to 8-week-old male C57BL/6J mice (Jackson Laboratory, Bar Harbor, ME; IMSR JAX:000664, RRID:IMSR_JAX:000664, **Figure 1A**). Mice were group-housed 5/cage in an AAALAC-approved facility at Children's Hospital of Philadelphia (CHOP). The vivariums at the Colket Translational Research Building (Penn/CHOP) are temperature- and humidity-controlled. Lights are on at 6 am and off at 6 pm, and food and water are provided *ad libitum*. All experiments were carried out in accordance with protocols approved by the Institutional Animal Care and Use Committee of CHOP and the guidelines established by the NIH Guide for the Care and Use of Laboratory Animals.

Craniectomy

All mice underwent craniectomy on day -1 of the experiment (Dixon et al., 1987; Smith et al., 2012). Mice were anesthetized with an intraperitoneal (i.p.) injection of ketamine (100 mg/kg)

and xylazine (6-16 mg/kg). Once anesthetized, mice were placed in a stereotaxic frame (Stoelting, Wood Dale, IL, United States), the scalp was incised and pulled away to fully expose the right parietal bone. An ultra-thin Teflon disk (3-mm outer diameter) was positioned between Lambda and Bregma and between the sagittal suture and the lateral ridge over the right hemisphere, and then glued to the skull with Vetbond (3M, St. Paul, MN, United States). Guided by the Teflon disk, a trephine was used to perform a 3-mm diameter craniectomy over the right parietal area. Following craniectomy, a Luer-lock needle hub (3-mm inner diameter) was secured above the skull opening with Loctite superglue and dental acrylic, filled with saline and capped. Mice were removed from the stereotaxic apparatus, placed on a heating pad until fully recovered from anesthesia, and then returned to their respective home cage.

Lateral Fluid Percussion Injury (LFPI)

Twenty-four hours (h) post-craniectomy, mice underwent LFPI or Sham surgery (**Figure 1A**; Dixon et al., 1987; Smith et al., 2012). Mice were placed under isoflurane anesthesia (2% oxygen, 500 ml/min) in a chamber. Respiration was visually monitored until mice reached a surgical plane of anesthesia (1 respiration/2 s). Mice were then removed from isoflurane and the needle hub was refilled with saline and connected to the fluid percussion injury device (Department of Biomedical Engineering, Virginia Commonwealth University) via high-pressure tubing. The mouse was placed onto a heating pad on its left side. On resumption of normal breathing pattern but before sensitivity to stimulation, the injury was induced by a 20-ms pulse of saline onto the intact dura. The pressure transduced onto the dura was monitored with an oscilloscope, with injury severity ranging from 1.4 to 1.6 atmospheres. Sham mice underwent all surgical procedures including attachment to the FPI device with exclusion of the actual fluid pulse. Immediately after injury or Sham surgery, the hub was removed from the skull and the mouse was placed in a supine position to measure the latency to righting. All mice in this study righted themselves within 3 min, while Sham mice righted themselves in <1 min. After righting, the mouse was returned to placement under isoflurane for scalp suturing. Mice recovered on a heating pad until mobile, at which point they were returned to their home cage. Within a cage, mice were exposed to either Sham or LFPI and post-surgery Sham and LFPI mice were housed in the same cage. Two cohorts of 5 Sham and 5 LFPI mice were generated for each condition at each time point (3, 7, and 31 days post-Sham or post-LFPI).

Bromodeoxyuridine (BrdU)

Administration

BrdU (Accurate Scientific, OBT0030G), a thymidine analog, was freshly prepared at 10mg/mL in 0.09% sterile saline and 0.007N NaOH. All mice received a single 150 mg/kg i.p. injection 3 days after Sham or LFPI (**Figure 1A**). Mice were weighed the morning of BrdU administration, and left undisturbed until BrdU injection was delivered that afternoon, and also were undisturbed for 2 h post-BrdU injection. In C57BL/6J male

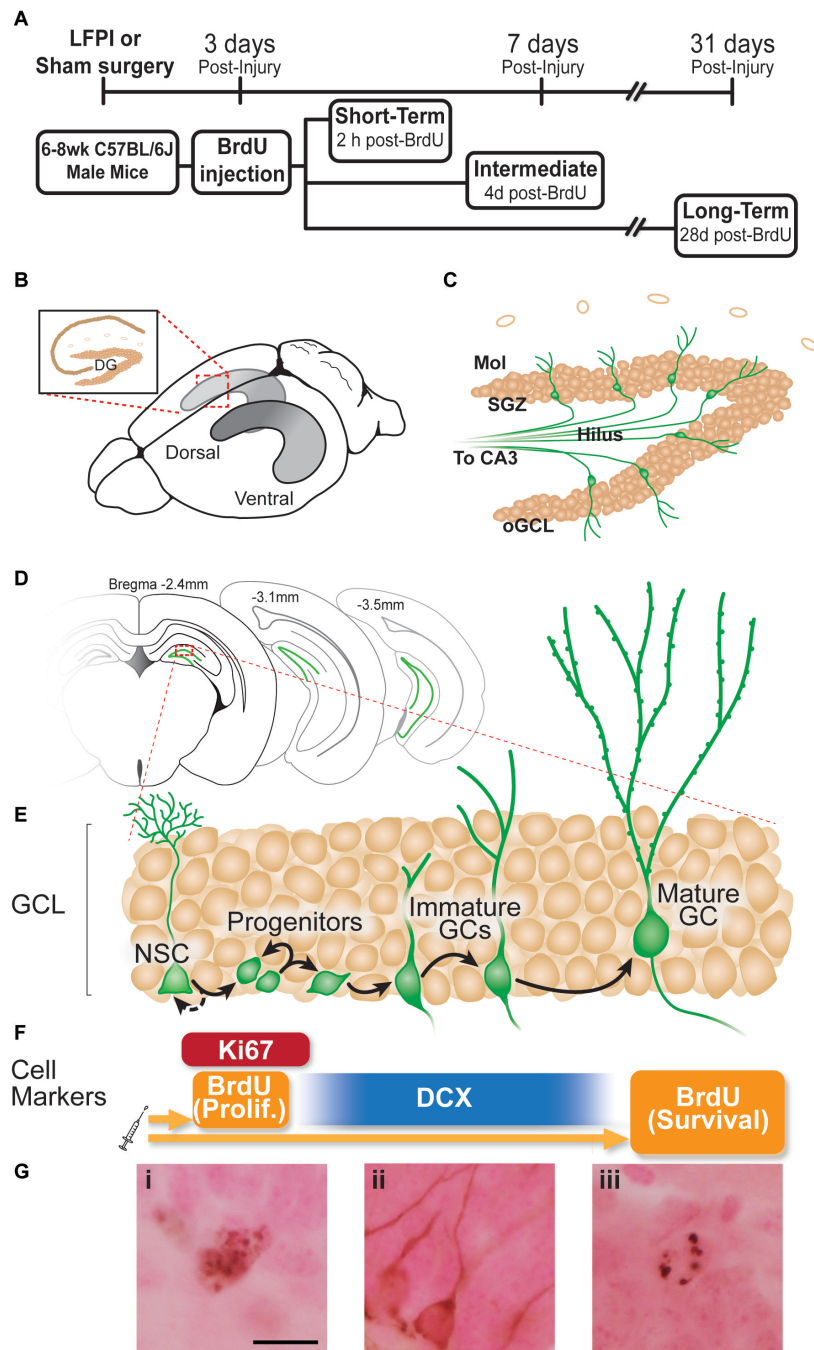


FIGURE 1 | Experimental timeline and overview of dentate gyrus (DG) neurogenesis and immunohistochemical markers used. **(A)** Timeline of experimental procedures. 6-8 week old male C57BL/6J mice received lateral fluid percussive injury (LFPI) or Sham surgery, and 150 mg/kg i.p. Bromodeoxyuridine (BrdU) injection 3 days post-injury (dpi). The Short-Term group was perfused 3 dpi (2 h post-BrdU); the Intermediate group perfused 7 dpi (4 days post-BrdU); and the Long-Term group perfused 31 dpi (28 days post-BrdU). **(B)** Schematic of a whole mouse brain showing bilateral location of the hippocampus (gray structure). Exploded inset (red dotted lines) depicts a coronal section through the dorsal hippocampus (tan indicates primary cell layers) with the granule cell layer (GCL) of the DG indicated. **(C)** Schematic of enlarged DG subregions. GCL is represented by densely packed tan circles; individual tan circles represent dorsal boundary of DG (hippocampal fissure). Green circles/lines are GCL GCs and their axons project through the Hilus to eventually reach CA3 (not pictured). Mol: molecular layer. SGZ: subgranular zone. oGCL: outer granule cell layer. **(D)** Schematic of location of DG (green lines) in coronal sections of a mouse brain at three distances from Bregma (-2.4, -3.1, and 4-3.5 mm). **(E, F)** Exploded inset of red dotted line in **(D)** depicts stages of GCL neurogenesis and the antibodies with which cells in each neurogenesis stage can be labeled. Neural stem cells (NSCs) asymmetrically divide to create progenitor cells, whose progeny differentiate into immature granule cells, some of which survive to become mature granule cells. BrdU (in the Short-Term group) and Ki67 (all groups) mark dividing cells; doublecortin (DCX) marks neuroblasts/immature neurons (in all groups); and BrdU in the Long-term group marks surviving cells (cells that were dividing and labeled at the time of BrdU injection, and have survived to 31 dpi). **(G)** Representative photomicrographs of cells stained with antibodies against Ki67 (Gi), DCX (Gii), or BrdU (Giii). Scale bar = 10 μ m.

mice, this BrdU dose and injection procedure “pulse-labels” cells in S-phase of the cell cycle at the time of BrdU injection (Mandyam et al., 2007).

Tissue Collection and Immunohistochemistry (IHC)

Three, 7, or 31 days post-Sham or -LFPI (**Figure 1**), mice were anesthetized with chloral hydrate (400 mg/kg, i.p.) prior to intracardial perfusion with ice-cold 0.1 M phosphate-buffered saline (PBS) for exsanguination followed by 4% paraformaldehyde for fixation (Rivera et al., 2013; DeCarolis et al., 2014). Extracted brains were immersed for 24 h in 4% paraformaldehyde in 0.1M PBS at 4°C for post-fixation, followed by least 3 days of immersion in 30% sucrose in 0.1 M PBS for cryoprotection with 0.01% sodium azide to prevent bacterial growth. For coronal brain sectioning, the brain of each mouse extending from anterior to the DG to the cerebellum (from 0.22 to $-5.34 \mu\text{m}$ from Bregma) was sectioned at $30 \mu\text{m}$ in a 1:9 series using a freezing microtome (Leica SM 2000 R Sliding Microtome). Sections were stored in 1xPBS with 0.01% sodium azide at 4°C until processing for IHC. Slide-mounted IHC for Ki67+, DCX+, and BrdU+ cells in the DG was performed as previously described (Rivera et al., 2013; DeCarolis et al., 2014). Briefly, one entire series of the hippocampus (every 9th section) was slide-mounted onto charged slides (Thermo Fisher Scientific, 12-550-15, Pittsburgh, PA, United States). Slide-mounted sections underwent antigen retrieval (0.01 M citric acid pH 6.9, 100°C, 15 min) followed by washing in 1xPBS at room temperature. For BrdU IHC, two additional steps were performed to allow the antibody access to DNA inside the cell nucleus: permeabilization (0.1% Trypsin in 0.1 M TRIS and 0.1% CaCl_2 , 10 min) and denaturation (2N HCl in 1x PBS, 30 min). Non-specific binding was blocked with 3% serum (donkey) and 0.3% Triton-X in PBS for 30 min. After blocking and pretreatment steps, sections were incubated with rat- α -BrdU (1:400; Accurate catalog OBT0030, Westbury, NY, United States), rabbit- α -Ki67 antibody (1:500; Thermo Fisher Scientific catalog RM-9106S, Fremont, CA, United States), or goat- α -DCX (1:4000; Santa Cruz Biotechnology catalog sc-8066, Dallas, TX, United States) in 3% serum and 0.3% Tween-20 overnight. For single labeling IHC, primary antibody incubation was followed by 1xPBS rinses, incubation with biotinylated secondary antibodies (biotin-donkey- α -rat-IgG, catalog 712-065-153; biotin-donkey- α -rabbit-IgG, catalog 711-065-152; or biotin-donkey- α -goat-IgG, catalog 705-065-003; all 1:200, all from Jackson ImmunoResearch, West Grove, PA, United States) for 1 h, and 1xPBS rinses. Next, endogenous peroxidase activity was inhibited via incubation with 0.3% hydrogen peroxide (H_2O_2) for 30 min, followed by incubation with an avidin-biotin complex for 60-90 min (ABC Elite, Vector Laboratories PK-6100). After another set of rinses in 1xPBS, immunoreactive cells were visualized via incubation with metal-enhanced diaminobenzidine (Thermo Fisher Scientific, 34065, Pittsburgh, PA, United States) for 5-10 min. Finally, slides were incubated for ~ 2 min in the nuclear counterstain, Fast Red (Vector Laboratories catalog H3403), dehydrated via a

series of increasing ethanol concentrations, and coverslipped using DPX (Thermo Fisher Scientific, 50-980-370, Pittsburgh, PA, United States).

Cavalieri Volume Estimation

Granule cell layer (GCL) volume was assessed using the Cavalieri Estimator Probe within the Stereo Investigator software (Gundersen et al., 1988; Harburg et al., 2007; Basler et al., 2017). All measurements were obtained using the Stereo Investigator software (MBF Bioscience, Williston, VT, United States) and a 40 \times objective (numerical aperture [NA] 0.75) on a Zeiss AxioImager M2 microscope. A $20 \mu\text{m}^2$ counting grid was superimposed over a live image of each section that contained the DG. This grid was used to calculate the area of the GCL at each distance from Bregma. Using the Cavalieri principle (Gundersen and Jensen, 1987; Gundersen et al., 1988), the area values were used to find the volume of the DG GCL.

Cell Type Quantification

Stereology was used to quantify indices relevant to the process of DG neurogenesis (Ki67+, DCX+, and BrdU+ cell number), as described in each subsection below and shown in **Figures 1B–G**.

Quantification of Ki67+ and BrdU+ Cells in the DG

Due to their rarity (Lagace et al., 2010), BrdU+ and Ki67+ cells were quantified exhaustively in the DG in every 9th section spanning the entire hippocampus via brightfield microscopy using a 40X objective (NA 0.90) on an Olympus BX 51 microscope. Factors considered in determining Ki67+ or BrdU+ cells were size, color, shape, transparency, location, and focal plane. BrdU+ and Ki67+ cells were quantified in 4 DG subregions: the SGZ ($40 \mu\text{m}$ into the hilus and the inner half of the GCL), widely considered to be the “neurogenic niche” of the DG (Riquelme et al., 2008; Zhao et al., 2008; Kezele et al., 2017; Oberner and Alvarez-Buylla, 2019); the outer GCL (oGCL), to which a minority of adult-generated cells migrate (Kempermann et al., 2003); the hilus, through which DG granule cells project their processes toward CA3; and the molecular layer, the site of DG granule cell dendrites and DG inputs from the entorhinal cortex. Resulting cell counts were multiplied by 9 to get total cell number.

Quantification of DCX+ Cells in the DG

DCX+ cells in the DG were quantified via unbiased stereology in only one region of interest (ROI): the SGZ and GCL proper (including the inner and oGCL). DCX+ cells in the oGCL were rare, and thus were considered part of the GCL. DCX+ cells in the hilus and molecular layer had ambiguous/faint staining with this and other antibodies, and thus DCX+ cells in these regions were not quantified. DCX+ cells in the SGZ/GCL are densely presented compared to the relatively rare populations of Ki67+ and BrdU+ cells; therefore, DCX+ cells in the SGZ/GCL were quantified using the optical fractionator workflow in StereoInvestigator (MicroBrightField, MBF) (Brown et al., 2003; Lagace et al., 2010; Zhao et al., 2010). Briefly, every 9th coronal section spanning the entire hippocampus

was analyzed on a Nikon Eclipse Ni or Zeiss AxioImager M2 microscope. The ROI (SGZ/GCL) was traced for each section at 100X magnification (10X objective, NA 0.30). Quantification was performed at 400X (40X objective, NA 0.75) by focusing through the Z-plane of the section. DCX+ cells were counted if they fulfilled three criteria: the entire boundary of the cell body was visible, there was a dendritic process emerging from the cell body, and the soma was darker than the surrounding background. DCX+ cells were only excluded on the basis of size if they were small enough to be a swelling of a dendrite (<~5 μ m).

Quantification of Ki67+, BrdU+, and DCX+ Cells Along the Longitudinal Axis (by Bregma)

For anterior/posterior analysis of Ki67+, BrdU+, and DCX+ cell number, results were divided into anterior and posterior bins, defined by a division at Bregma level -2.60 mm (Tanti et al., 2012; Tanti and Belzung, 2013; Zhou et al., 2016). Bregma level -2.60 mm was identified based on when hippocampal CA3 reaches approximately halfway down the dorsal/ventral extent of the brain, and the corpus callosum no longer connects the left and right hemispheres (Paxinos and Franklin, 2019). Cell counts for each section anterior to -2.60 mm were summed and multiplied by 9 to get an anterior value for each mouse. The same procedure was used for the posterior analysis, using all sections posterior to Bregma level -2.60 mm.

Data Presentation and Analysis and Image Presentation

Experimenters were blinded to injury condition, and code was only broken after data analyses were complete. Counts for cellular markers were collected for at least 5 (cohort 1) and at most 10 (cohorts 1 and 2) Sham and LFPI mice at the 3, 7, and 31-dpi time points. Due to the pandemic-decreed, multi-month lab shut-down, not every cellular marker at each time point was analyzed in both cohorts. However, for cellular markers that were quantified in both cohorts, the data from each cohort were pooled together after confirmation of no cohort variance. Data are presented as individual data points with mean and standard error of the mean displayed. Data were assessed for normality with the Shapiro-Wilk test. Normal data were analyzed with unpaired two-tailed t-test, and non-normal data were analyzed with the Mann-Whitney test. Graphs were generated in GraphPad Prism (version 8.0). Full details of statistical analyses for each figure panel are provided in **Supplementary Tables 1, 2**. Photomicrographs were taken with an Olympus DP74 camera using CellSens Standard software, or a Zeiss Lumina HR color camera using MBF StereoInvestigator software, and imported into Adobe Illustrator (version 24.3) for cropping and labeling. For photomicrographs in **Figures 2, 4, 6**, representative images from similar Bregma levels are provided when the difference between Sham and LFPI cell numbers was significant. For **Figures 3, 5, 7**, a schematic of the DG with a given subregion outlined in red is included to the left of the corresponding cell counts.

RESULTS

Weight and Gross Locomotor Activity 3, 7, and 31 Dpi

This LFPI mouse model of mild TBI (Dixon et al., 1987; Smith et al., 2012) did not change weight or weight gain between Sham and LFPI mice at the three time points examined: 3, 7, or 31 dpi (**Figure 1A**; data not shown). Observation several hours prior to perfusion at each time point by an experimenter blinded to injury condition did not reveal gross differences in locomotor activity between Sham and LFPI mice.

Three Dpi: Neurogenesis Indices in the Ipsilateral DG Neurogenic Regions

Three days was selected as the earliest time point post-Sham or post-LFPI to quantify indices of DG neurogenesis (proliferation and neuroblasts/immature neurons). This was for two reasons. First, DG function and neurogenesis are commonly studied 7 dpi (Gilley and Kernie, 2011; Sun et al., 2015; Ibrahim et al., 2016; Neuberger et al., 2017; Shapiro, 2017; Carlson and Saatman, 2018; Wu et al., 2018; Aleem et al., 2020), a time point when the DG is hyperexcitable and DG-dependent spatial memory is impaired (Folweiler et al., 2018). DG neurogenesis influences both DG excitability and DG-dependent behavior (Lacefield et al., 2012; Ikrar et al., 2013; Park et al., 2015; Neuberger et al., 2017). Therefore, examination of neurogenesis indices 3 dpi may reveal changes that influence the subsequent emergence of 7 dpi DG hyperexcitability and functional impairment. Second, indices of DG proliferation and neurogenesis are changed 3 dpi in more severe TBI models relative to control animals (Dash et al., 2001; Chirumamilla et al., 2002; Peters et al., 2018; Villasana et al., 2019), but only a few papers look at DG neurogenesis at a short-term time point post-mTBI, and the results are mixed (Wang et al., 2016; Neuberger et al., 2017; Tomura et al., 2020). To address this knowledge gap, the neurogenic regions of the DG (SGZ, GCL) from Sham and LFPI mice were assessed 3 dpi for indices of proliferation (Ki67+ and BrdU+ cell number) and neuroblasts/immature neurons (DCX+ cell number).

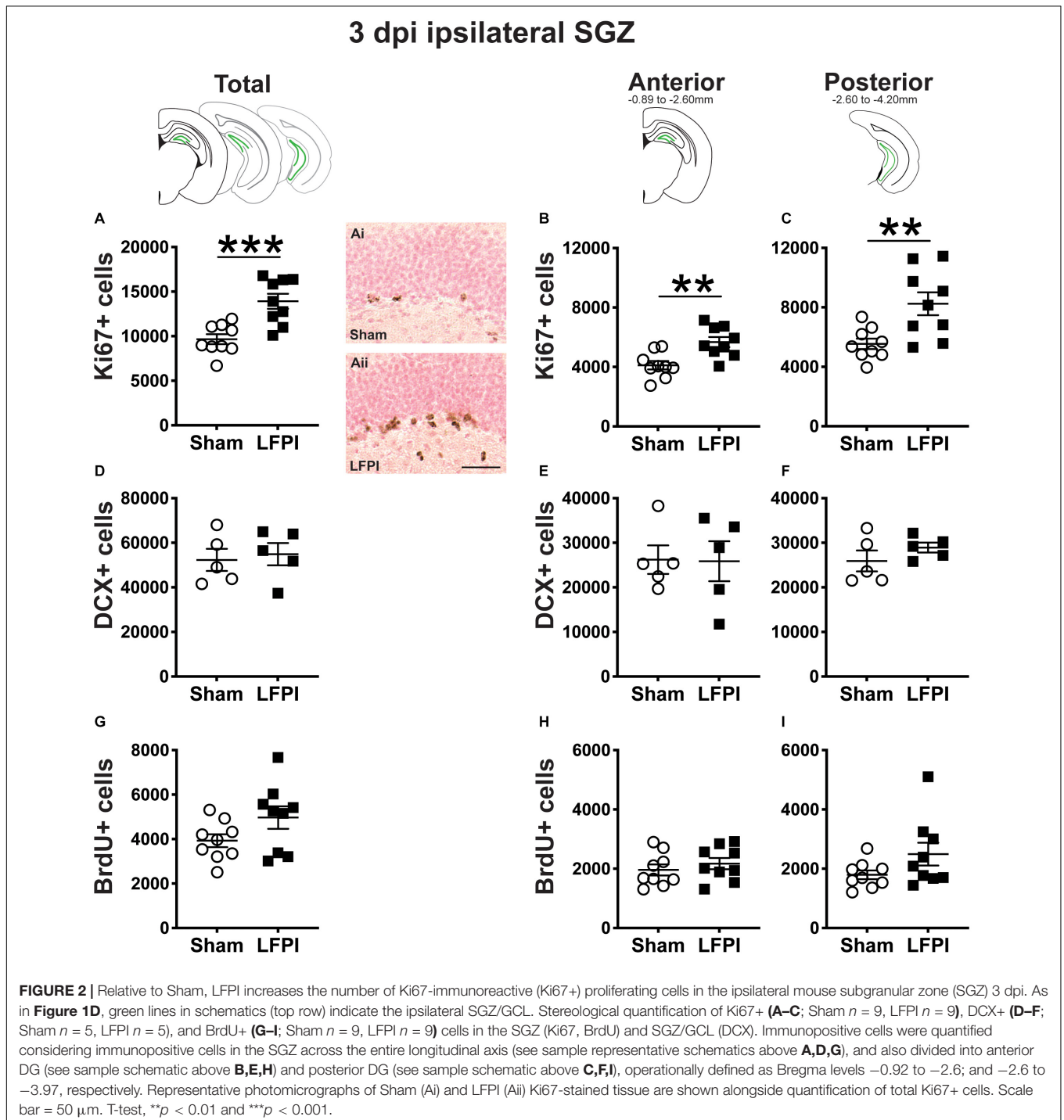
Three Dpi, There Are More Ki67+ Proliferating Cells (Cells in the Cell Cycle) in the Ipsilateral Neurogenic Region (SGZ) in LFPI Mice Relative to Sham Mice

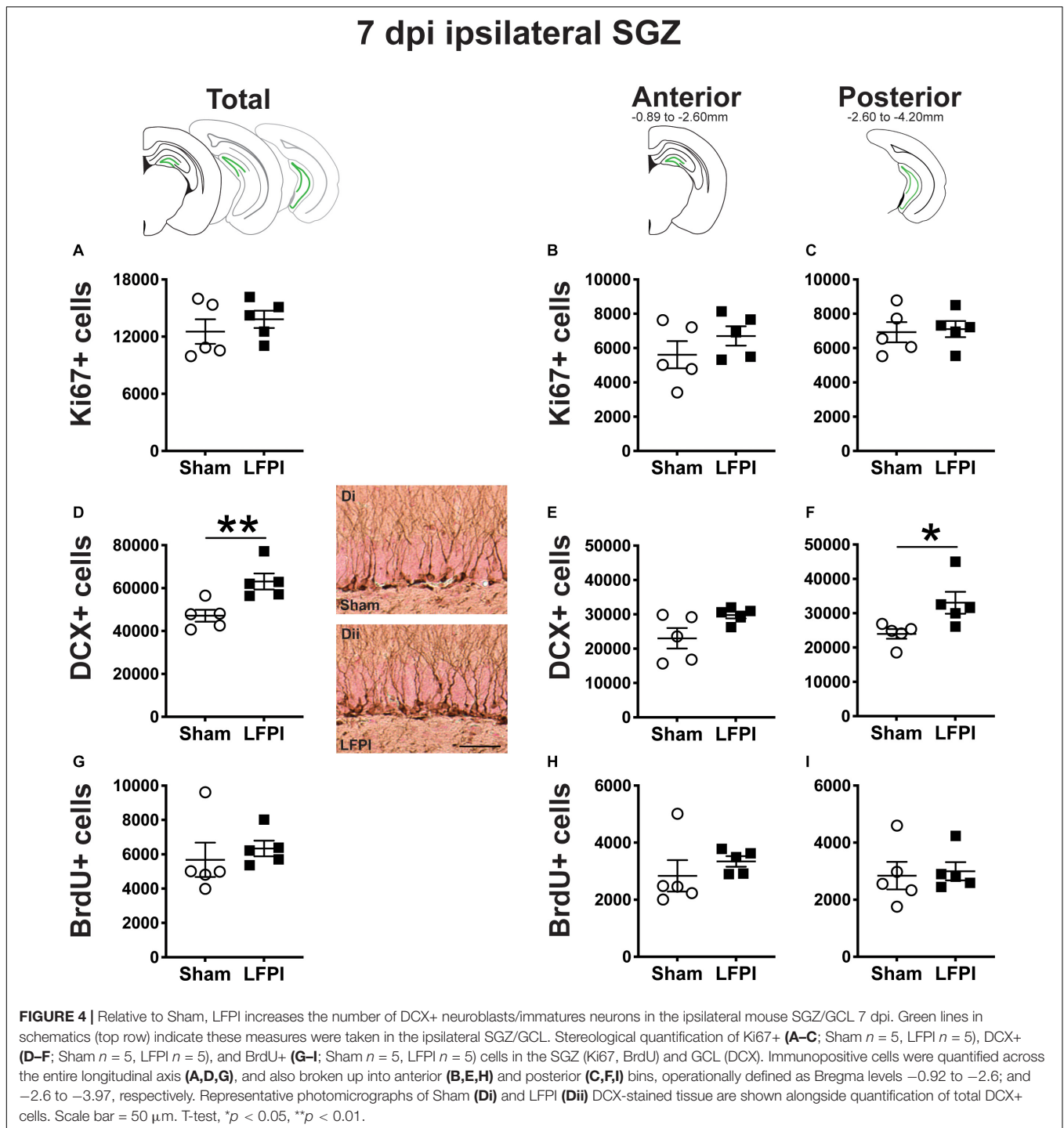
Ki67 is an endogenous protein with a short half-life expressed in all cells that are in stages of the cell cycle (G1, S, G2, M) (Brown and Gatter, 2002). Ki67+ cells in the adult mouse SGZ are thus in the cell cycle or “proliferating” at the time of tissue collection (Mandyam et al., 2007), which is in keeping with the clustering of Ki67+ nuclei seen in the SGZ of both Sham and LFPI mice (**Figures 1E,Gi**). Stereological assessment of Ki67+ SGZ cells mice 3 dpi revealed an effect of injury (**Figure 2A**), with ~45% more Ki67+ SGZ cells in LFPI vs. Sham mice (statistics for this and all subsequent measures provided in **Supplementary Tables 1, 2**). As the DG, and thus the SGZ, varies along its longitudinal axis in regard to afferents, efferents, and function (Scharfman, 2011; Wu et al., 2015; Levone et al., 2020), Ki67+ cells

were also quantified in the anterior vs. posterior SGZ with the division defined as -2.60mm relative to Bregma (Tanti and Belzung, 2013). Similar to the analysis on the entire SGZ (Figure 2A), analysis of Ki67+ cell number in the anterior and posterior SGZ 3 dpi revealed an effect of injury, with $\sim 40\%$ (Figure 2B) and $\sim 50\%$ more Ki67+ cells (Figure 2C), respectively, in the ipsilateral neurogenic SGZ of LFPI vs. Sham mice.

Three Dpi, the Number of DCX+ Neuroblasts/Immature Neurons in the Ipsilateral Mouse SGZ/GCL Is Similar Between Sham and LFPI Mice

The SGZ/GCL of Sham and LFPI mice was examined for cells expressing DCX, a microtubule-associated protein expressed in late progenitor cells (neuroblasts) and immature neurons (Francis et al., 1999; Nacher et al., 2001;





Couillard-Despres et al., 2005; La Rosa et al., 2019). DCX+ cells were quantified in both SGZ and GCL as DCX+ cells with neurogenic potential are clearly identifiable in both these DG subregions in control tissue. In the SGZ/GCL of Sham and LFPI mice collected 3 dpi, there was no effect of injury on total DCX+ cell number (**Figure 2D**). When the SGZ/GCL in Sham and LFPI mice 3 dpi was divided into anterior and posterior sections, there was also no effect of injury on DCX+

cell number in either the anterior (**Figure 2E**) or posterior (**Figure 2F**) bin.

Three Dpi, the Number of Proliferating Cells (Cells in S Phase of the Cell Cycle) in the Ipsilateral Mouse SGZ Is Similar Between Sham and LFPI Mice

Finally, the SGZ of Sham and LFPI mice was analyzed for cells immunopositive for BrdU, a thymidine analog administered to

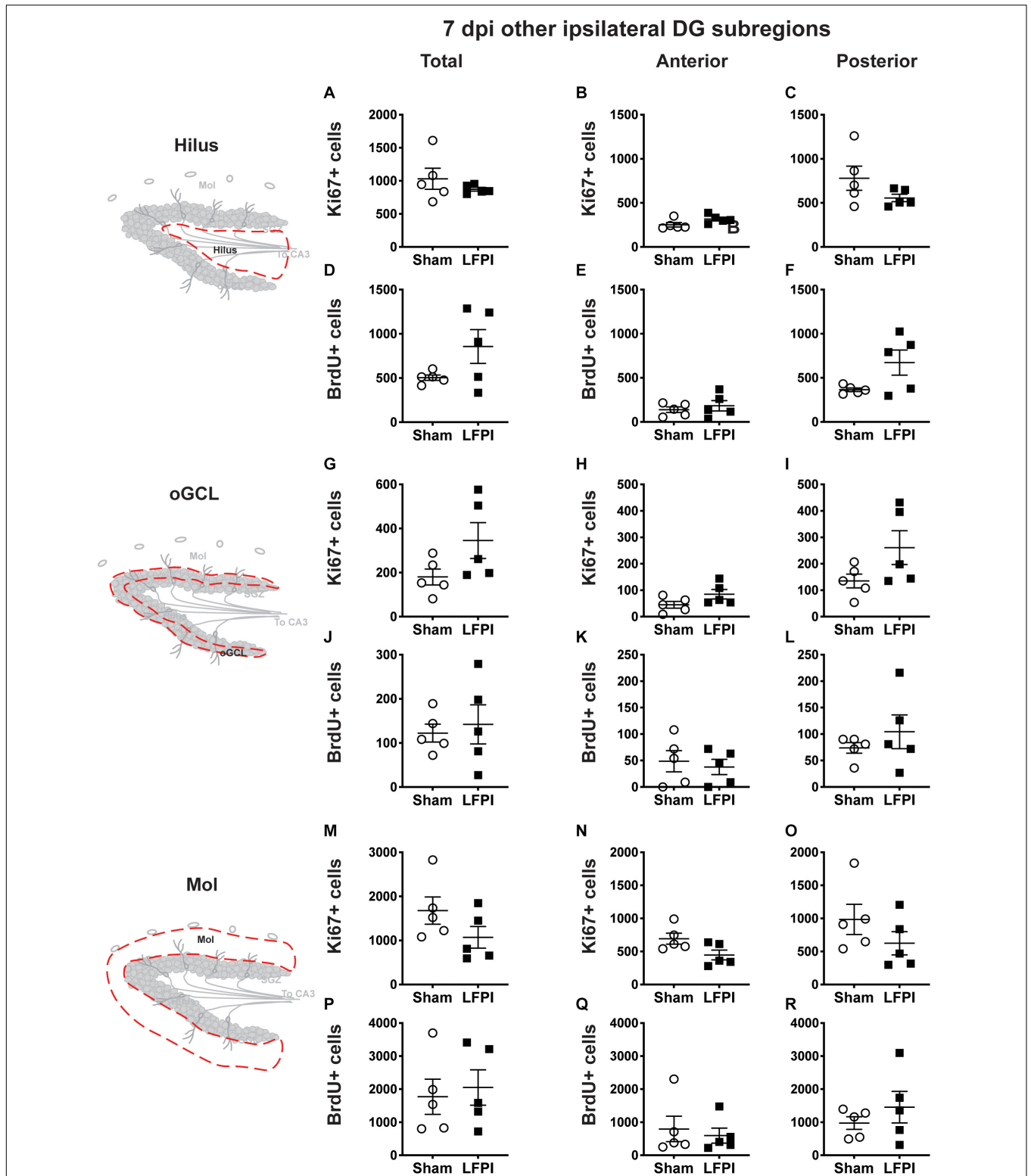
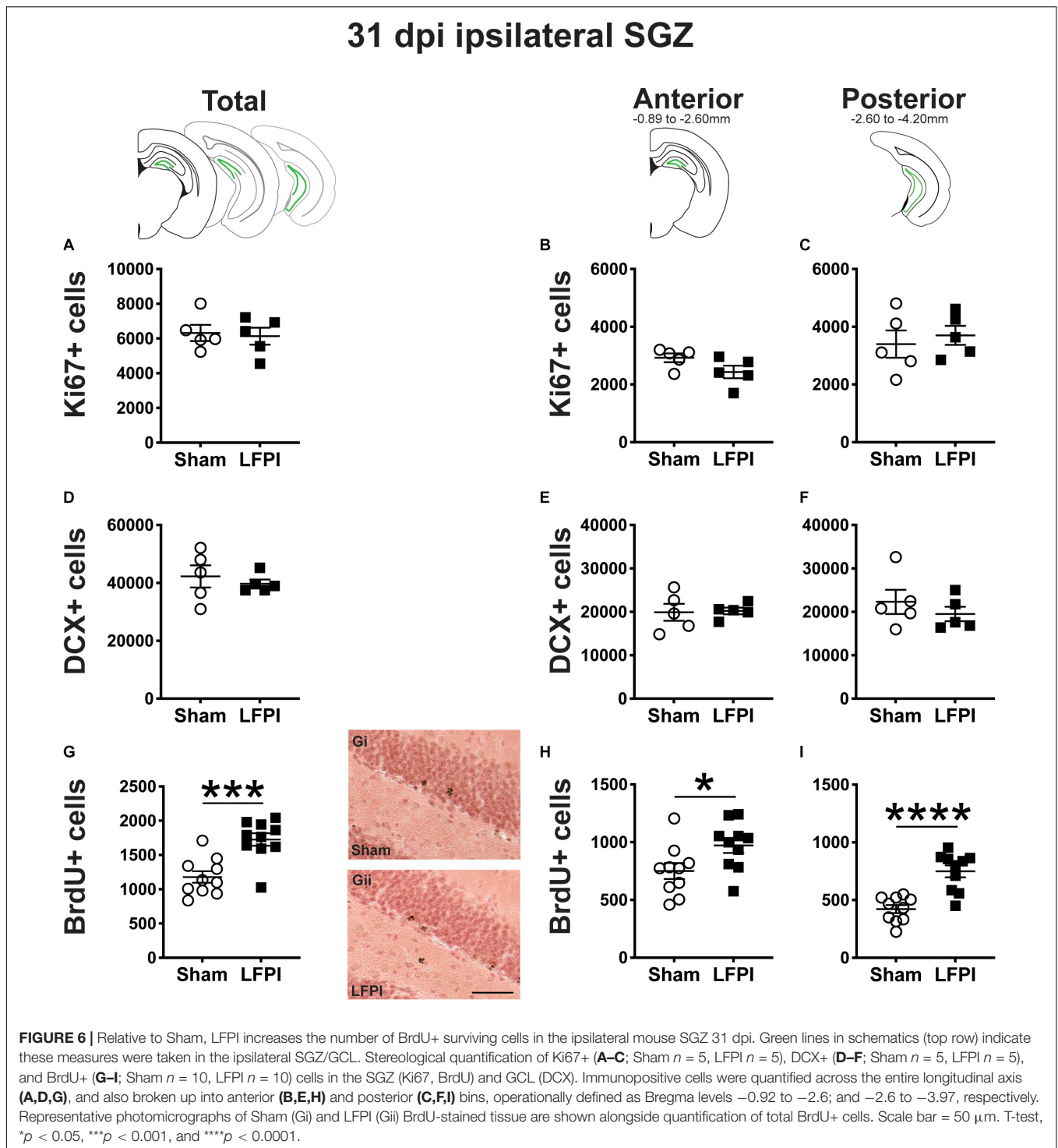


FIGURE 5 | Relative to Sham, LFPI does not change the number of Ki67+ or BrdU+ cells in the ipsilateral DG hilus, oGCL, and Mol 7 dpi. Stereological quantification of Ki67+ (**A–C,G–I,M–O**; Sham $n = 5$, LFPI $n = 5$) and BrdU+ (**D–F,J–L,P–R**; Sham $n = 5$, LFPI $n = 5$) cells in the hilus (**A–F**; red dotted line region, top-left schematic), outer granule cell layer (**G–L**; red dotted line region, middle-left schematic), and molecular layer (**M–R**; red dotted line region, bottom-left schematic). Immunopositive cells were quantified across the entire longitudinal axis (**A,D,G,J,M,P**), and also broken up into anterior (**B,E,H,K,N,Q**), and posterior (**C,F,I,L,O,R**) bins, operationally defined as Bregma levels -0.92 to -2.6 ; and -2.6 to -3.97 , respectively.



all mice 3 dpi. BrdU integrates into the DNA of cells in the S phase of the cell cycle at the time of BrdU injection. The short *in vivo* bioavailability of BrdU in mice (<15 min, Mandyam et al., 2007) allows a “pulse” labeling of cycling cells and the ability to track them and their progeny over time. In the ipsilateral SGZ of Sham and LFPI mice collected 3 dpi (2 h post-BrdU injection, Short-Term group, **Figures 1A,F**), there was no effect of injury

(**Figure 2G**). Parcellation of Sham and LFPI BrdU+ SGZ cell counts into anterior and posterior DG bins also showed no effect of injury (**Figures 2H,I**). While both Ki67 and short-term BrdU were examined as indices of proliferation in the SGZ, they do not represent the same cell population; exogenous BrdU “pulse” labels cells in S-phase, while Ki67 is an endogenous marker of cells in G1, S, G2, and M phase. Thus, despite the lack of

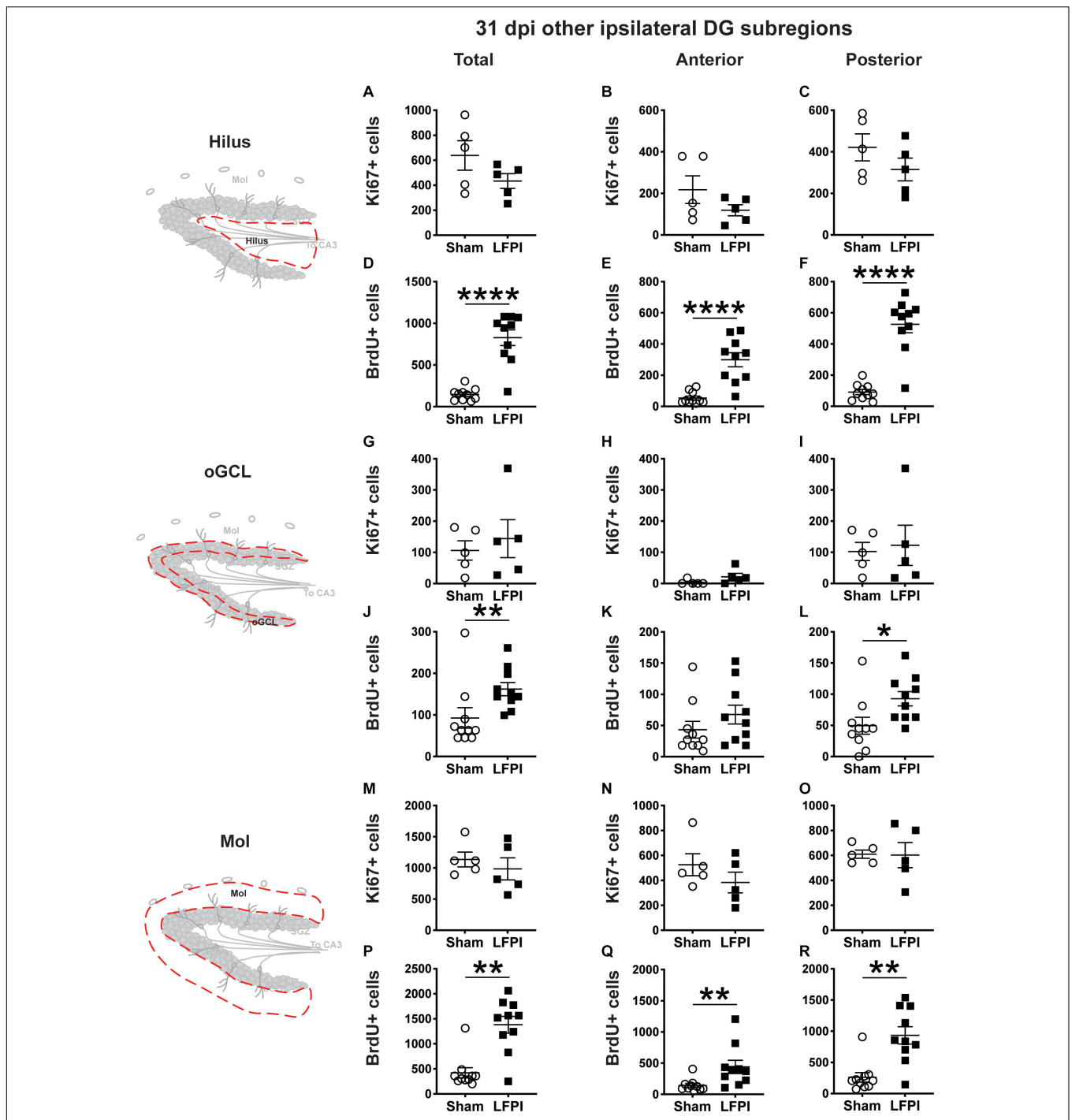


FIGURE 7 | Relative to Sham, LFPI increases the number of BrdU+ surviving cells in the ipsilateral DG hilus, posterior oGCL, and Mol 31 dpi. Stereological quantification of Ki67+ (A–C, G–I, M–O; Sham $n = 5$, LFPI $n = 5$) and BrdU+ (D–F, J–L, P–R; Sham $n = 10$, LFPI $n = 10$) cells in the hilus (A–F; red dotted line region, top-left schematic), outer granule cell layer (G–L; red dotted line region, middle-left schematic), and molecular layer (M–R; red dotted line region, bottom-left schematic). Immunopositive cells were quantified across the entire longitudinal axis (A, D, G, J, M, P), and also broken up into anterior (B, E, H, K, N, Q) and posterior (C, F, I, L, O, R) bins, operationally defined as Bregma levels -0.92 to -2.6 ; and -2.6 to -3.97 , respectively. T-test, * $p < 0.05$, ** $p < 0.01$, and **** $p < 0.0001$.

change in SGZ BrdU+ cell number between Sham and LFPI mice (which suggests the number of cells in S phase does not change 3 dpi), the greater number of Ki67+ cells in LFPI vs.

Sham mice suggests the number of proliferating cells in the entire cell cycle is increased in the ipsilateral SGZ of LFPI mice 3 dpi relative to Sham.

Three Dpi: Neurogenesis Indices in the Contralateral DG Neurogenic Regions

Our main focus for this study was comparing indices of proliferation and neurogenesis in neurogenic regions in the hemisphere ipsilateral to the injury in Sham and LFPI mice, in keeping with the common approach in studies of unilateral injury. However, as the left and right mouse DG are neuroanatomically connected, and as some TBI studies examine or even compare neurogenesis indices between the ipsilateral and contralateral hemispheres (Tran et al., 2006; Gao et al., 2008; Blaiss et al., 2011; Zhou et al., 2012; Hood et al., 2018), we also quantified these indices in the SGZ contralateral to the injury in Sham and LFPI mice.

Three Dpi, Ki67+ Cell Number Is Similar in the Contralateral SGZ Between Sham and LFPI Mice

In contrast to the Ki67+ cell results from the ipsilateral hemisphere (where there are more Ki67+ cells in LFPI vs. Sham SGZ 3 dpi, **Figures 2A–C**), in the contralateral SGZ 3 dpi there was no effect of injury on total Ki67+ cell number (**Supplementary Figure 1A**) and no effect of injury on Ki67+ cell number in either the anterior or posterior contralateral SGZ (**Supplementary Figures 1B,C**).

Three Dpi, DCX+ Cell Number Is Similar in the Contralateral SGZ/GCL Between Sham and LFPI Mice

Similar to the DCX+ cell results from the ipsilateral hemisphere (**Figures 2D–F**), in the contralateral SGZ/GCL there was no effect of injury on total DCX+ cell number 3 dpi (**Supplementary Figure 1D**) and no effect of injury on DCX+ cell number in either the anterior or posterior contralateral SGZ/GCL (**Supplementary Figures 1E,F**).

Three Dpi, BrdU+ Cell Number (Cells in S Phase of the Cell Cycle) Is Similar in the Contralateral SGZ Between Sham and LFPI Mice

Similar to the BrdU+ cell results from the ipsilateral hemisphere (**Figures 2G–I**), in the contralateral SGZ there was no effect of injury on total BrdU+ cell number 3 dpi (**Supplementary Figure 1G**) and no effect of injury on BrdU+ cell number in either the anterior or posterior contralateral SGZ (**Supplementary Figures 1H,I**).

Three Dpi: Proliferation Indices in the Ipsilateral and Contralateral DG Non-neurogenic Regions

In naive rodents, new neurons primarily emerge from the main DG neurogenic region: the SGZ/inner portion of the GCL; it is rare for other DG subregions (hilus, oGCL, molecular layer) to give rise to new neurons. However, in naive rodents, these “non-neurogenic” subregions contain proliferating cells (García-Martínez et al., 2020). Notably, proliferation in these non-neurogenic DG regions is often

different in injured vs. sham rodents in both the ipsilateral and contralateral hemispheres (Cho et al., 2015; Du et al., 2017; Neuberger et al., 2017). While these injury-induced changes in proliferation in non-neurogenic DG regions may reflect division of precursors of glia, not neurons (Avedaño and Cowan, 1979; Dragunow et al., 1990; Hailer et al., 1999; Blümcke et al., 2001; Littlejohn et al., 2020), the impact of glia on DG structure and function stress the importance of understanding how mTBI influences these measures. Therefore, 3 dpi the ipsilateral and contralateral hilus, oGCL, and molecular layer from Sham and LFPI mice were assessed for indices of proliferation (Ki67+ and BrdU+ cell number). For DCX+ neuroblasts/immature neurons, the oGCL DCX+ cells were considered as part of the SGZ/GCL analysis (**Figures 2D–F** and **Supplementary Figures 1D–F**); due to the presence of faint or ambiguous DCX+ cells in the hilus and molecular layer with this and other DCX+ antibodies in both experimental and control groups, DCX+ cells were not quantified in the hilus or molecular layer.

Three Dpi, There Are More Proliferating (Ki67+ and BrdU+ Cells) in Ipsilateral Non-SGZ DG Subregions in LFPI Mice Relative to Sham Mice

In the ipsilateral hilus 3 dpi, there was an effect of injury on total Ki67+ cells (**Figure 3A**) and BrdU+ cells (**Figure 3D**), with 135% and 130% more Ki67+ and BrdU+ cells, respectively, in LFPI vs. Sham mice. In the ipsilateral hemisphere, parcellation of Sham and LFPI BrdU+ hilus cell counts into anterior and posterior DG bins revealed significant effects of injury for both Ki67+ and BrdU+ cells in the anterior and posterior hilus. In the ipsilateral hemisphere, LFPI mice had 100% more anterior Ki67+ cells (**Figure 3B**), 150% more posterior Ki67+ cells (**Figure 3C**), 90% more anterior BrdU+ cells (**Figure 3E**), and 150% more posterior BrdU+ cells (**Figure 3F**) in the hilus vs. Sham mice. In the ipsilateral oGCL 3 dpi, there was also an effect of injury on Ki67+ cells, with 275% more total (**Figure 3G**), 260% more anterior (**Figure 3H**), and ~290% more posterior (**Figure 3I**) Ki67+ cells in LFPI vs. Sham mice. However, in the ipsilateral oGCL 3 dpi, there was no effect of injury on total BrdU+ oGCL cells (**Figure 3J**) or on anterior or posterior BrdU+ oGCL cells (**Figures 3K,L**). In the ipsilateral molecular layer 3 dpi, there was an effect of injury on total Ki67+ (**Figure 3M**) and BrdU+ (**Figure 3P**) cells, with 240% and 160% more Ki67+ and BrdU+ cells, respectively, in LFPI vs. Sham mice. In the ipsilateral parcellation of Sham and LFPI BrdU+ molecular layer cell counts into anterior and posterior DG bins revealed significant effects of injury with 250% more anterior Ki67+ (**Figure 3N**), 230% more posterior Ki67+ (**Figure 3O**), 80% more anterior BrdU+ (**Figure 3Q**), and 270% more posterior BrdU+ cells (**Figure 3R**) cells in the molecular layer of LFPI vs. Sham mice. These results show 3 dpi there is increased proliferation in the ipsilateral dentate gyrus in DG subregions that are classically believed to be non-neurogenic.

Three Dpi, There Are More Proliferating Ki67+ Cells in Some Contralateral Non-SGZ DG Subregions in LFPI Mice Relative to Sham Mice

In the contralateral hilus 3 dpi, there was an effect of injury on Ki67+ cells, with 65% more total (**Supplementary Figure 2A**) and 50% more posterior (**Supplementary Figure 2C**) Ki67+ cells in LFPI vs. Sham mice; the number of Ki67+ cells in the contralateral anterior hilus was similar between Sham and LFPI mice (**Supplementary Figure 2B**). There was no effect of injury on total (**Supplementary Figure 2D**) or anterior or posterior (**Supplementary Figures 2E,F**) BrdU+ cell number in the contralateral hilus 3 dpi. In the contralateral oGCL 3 dpi, there was an effect of injury on Ki67+ cells, with 475% more total (**Supplementary Figure 2G**) and 520% more posterior (**Supplementary Figure 2I**) Ki67+ cells in LFPI vs. Sham mice; as in the contralateral hilus, Ki67+ cell number in the contralateral anterior oGCL was similar between Sham and LFPI mice 3 dpi (**Supplementary Figure 2H**). There was no effect of injury on total (**Supplementary Figure 2J**) or anterior (**Supplementary Figure 2K**) BrdU+ cells, but there were 75% fewer BrdU+ cells in the contralateral posterior oGCL (**Supplementary Figure 2L**) in LFPI vs. Sham mice 3 dpi. In the contralateral molecular layer 3 dpi, there was no effect of injury on Ki67+ cell number (total **Supplementary Figure 2M**; anterior and posterior **Supplementary Figures 2N,O**) or BrdU+ cell number (total **Supplementary Figure 2P**, anterior and posterior **Supplementary Figures 2Q,R**) 3 dpi. These results show 3 dpi there is increased proliferation in the contralateral hilus and oGCL in LFPI vs. Sham mice, suggesting the influence of mTBI on proliferation is not restricted to the ipsilateral neurogenic and non-neurogenic regions. As in the ipsilateral 3 dpi analyses, in the contralateral 3 dpi analysis there is a disconnect between the impact of mTBI on the number of cells in S phase (BrdU+ cells, which are similar between Sham and LFPI in all contralateral DG subregions, with the exception of fewer BrdU+ cells in the oGCL in LFPI vs. Sham mice) and on cells in the entire cell cycle (Ki67+ cells, which are similar between Sham and LFPI in the contralateral SGZ but increased in the contralateral hilus and oGCL in LFPI vs. Sham mice).

Seven Dpi: Neurogenesis Indices in the Ipsilateral DG Neurogenic Regions

The same markers examined in ipsilateral 3 dpi DG were also analyzed in the ipsilateral DG of brains collected 7 dpi (**Figure 4**). Since all mice received a BrdU injection 3 dpi, by 7 dpi these BrdU+ cells represent cells that were in S-phase of the cell cycle 4 days prior, but may no longer be actively proliferating (Cameron and McKay, 2001; Dayer et al., 2003; Mandyam et al., 2007).

Seven Dpi, There Are the Same Number of Ki67+ Proliferating Cells in the Ipsilateral SGZ in LFPI and Sham Mice

In the ipsilateral SGZ of Sham and LFPI mice 7 dpi, there was no effect of injury on total Ki67+ cell number (**Figure 4A**). When divided into anterior/posterior bins, there was no effect of

injury on Ki67+ cell number in either the anterior (**Figure 4B**) or posterior (**Figure 4C**) ipsilateral SGZ 7 dpi.

Seven Dpi, There Are More DCX+ Neuroblasts/Immature Neurons in the Ipsilateral Mouse SGZ/GCL in LFPI Mice Relative to Sham Mice

In the ipsilateral SGZ/GCL of Sham and LFPI mice 7 dpi, there was an effect of injury (**Figure 4D**), with ~35% more total DCX+ SGZ/GCL cells in LFPI vs. Sham mice. When divided into anterior/posterior bins, there was no effect of injury on DCX+ cell number in the ipsilateral anterior SGZ/GCL (**Figure 4E**), but there was an effect of injury on DCX+ cell number in the ipsilateral posterior SGZ/GCL (**Figure 4F**) with ~40% more DCX+ SGZ/GCL cells in LFPI vs. Sham mice 7 dpi.

Seven Dpi, the Number of BrdU+ Cells (Cells in S Phase 4 Days Prior) in the Ipsilateral Mouse SGZ Is Similar Between Sham and LFPI Mice

In the ipsilateral SGZ of Sham and LFPI mice 7 dpi, there was no effect of injury on total BrdU+ cell number (**Figure 4G**). When divided into anterior/posterior bins, there was no effect of injury on BrdU+ cell number in either the anterior (**Figure 4H**) or posterior (**Figure 4I**) ipsilateral SGZ 7 dpi.

Seven Dpi: Neurogenesis Indices in the Contralateral DG Neurogenic Regions

Seven Dpi, the Number of Ki67+ Proliferating Cells in the Contralateral SGZ Is Similar Between Sham and LFPI Mice

In the contralateral SGZ of Sham and LFPI mice 7 dpi, there was no effect of injury on total Ki67+ cell number (**Supplementary Figure 3A**) or on Ki67+ cell number in the anterior (**Supplementary Figure 3B**) or posterior (**Supplementary Figure 3C**) contralateral SGZ.

Seven Dpi, the Number of BrdU+ Cells (Cells in S Phase 4 Days Prior) in the Contralateral SGZ Is Similar Between Sham and LFPI Mice

In the contralateral SGZ of Sham and LFPI mice 7 dpi, there was no effect of injury on total BrdU+ cell number (**Supplementary Figure 3A**) or on BrdU+ cell number in either the anterior (**Supplementary Figure 3B**) or posterior (**Supplementary Figure 3C**) contralateral SGZ.

Seven Dpi: Proliferation Indices in the Ipsilateral and Contralateral DG Non-SGZ Regions

Seven Dpi, the Numbers of Ki67+ Proliferating Cells and BrdU+ Cells (Cells in S Phase 4 Days Prior) in the Ipsilateral Non-SGZ DG Subregions Are Similar in Sham and LFPI Mice

In the ipsilateral DG 7 dpi, there was no effect of injury on Ki67+ cell number in the total hilus, oGCL, or Mol (**Figures 5A,G,M**) or in the anterior or posterior hilus, oGCL, or Mol (**Figures 5B,C,H,I,N,O**). Similarly, in the ipsilateral DG 7 dpi, there was no effect of injury on BrdU+ cell number in the

total hilus, oGCL, or Mol (Figures 5D,J,P) or in the anterior or posterior hilus, oGCL, or Mol (Figures 5E,F,K,L,Q,R).

Seven Dpi, the Numbers of Ki67+ Proliferating Cells and BrdU+ Cells (Cells in S Phase 4 Days Prior) in the Contralateral non-SGZ DG Subregions Are Similar in Sham and LFPI Mice

In the contralateral DG 7 dpi, there was no effect of injury on Ki67+ cell number in the total hilus, oGCL, or Mol (Supplementary Figures 4A,G,M) or in the anterior or posterior hilus, oGCL, or Mol (Supplementary Figures 4B,C,H,I,N,O). Similarly, in the contralateral DG 7 dpi, there was no effect of injury on BrdU+ cell number in the total hilus, oGCL, or Mol (Supplementary Figures 4D,J,P) or in the anterior or posterior hilus, oGCL, or Mol (Supplementary Figures 4E,F,K,L,Q,R).

Thirty-One Dpi: Neurogenesis Indices in the Ipsilateral DG Neurogenic Regions

The same markers examined in 3 and 7 dpi ipsilateral tissue were also analyzed in tissue harvested 31 dpi (Figure 4). BrdU+ cells 31 dpi reflect cells that were in S-phase of the cell cycle 28 days prior.

Thirty-One Dpi, the Number of Ki67+ Proliferating Cells in the Ipsilateral Mouse SGZ Is Similar Between Sham and LFPI Mice

In the ipsilateral SGZ 31 dpi, there was no effect of injury on Ki67+ cell number in the total (Figure 6A) or the anterior or posterior SGZ (Figures 6B,C). Given the cell cycle length of mouse SGZ cells and the dilution of BrdU that occurs with additional cell division (Cameron and McKay, 2001; Dayer et al., 2003; Mandyam et al., 2007), detectable BrdU+ SGZ cells 31 dpi are unlikely to be still proliferating, and thus here are interpreted as surviving cells.

Thirty-One Dpi, the Number of DCX+ Neuroblasts/Immature Neurons in the Ipsilateral Mouse SGZ/GCL Is Similar Between Sham and LFPI Mice

In the ipsilateral DG 31 dpi, there was no effect of injury on DCX+ cell number in the total (Figure 6A) or the anterior or posterior SGZ/GCL (Figures 6B,C).

Thirty-One Dpi (28 Days Post-BrdU Injection), the Number of BrdU+ Cells in the Ipsilateral Mouse SGZ Is Greater in LFPI vs. Sham Mice

In the ipsilateral DG 31 dpi, there was an effect of injury on BrdU+ cell number in the total SGZ (Figure 6G), with ~45% more cells in LFPI vs. Sham mice. When divided into anterior/posterior bins, there was also an effect of injury with ~30% (Figure 6H) and ~75% more BrdU+ cells (Figure 6I), respectively, in LFPI vs. Sham mice (Figures 6B,C). These data suggest that all the number of cells in S-phase is unchanged when BrdU is first injected (Figures 2G-I), survival of those BrdU+ cells and/or their progeny is increased in LFPI mice by 31 dpi vs. Sham mice.

Thirty-One Dpi: Neurogenesis Indices in the Contralateral DG Neurogenic Regions

Thirty-One Dpi, the Number of Ki67+ Proliferating Cells in the Contralateral SGZ Is Similar Between Sham and LFPI Mice

In the contralateral SGZ of Sham and LFPI mice 31 dpi, there was no effect of injury on total Ki67+ cell number (Supplementary Figure 5A) or on Ki67+ cell number in the anterior (Supplementary Figure 5B) or posterior (Supplementary Figure 5C) contralateral SGZ.

Thirty-One Dpi, the Number of DCX+ Immature Neurons/Neuroblasts in the Contralateral SGZ/GCL Is Similar Between Sham and LFPI Mice

In the contralateral SGZ/GCL of Sham and LFPI mice 31 dpi, there was no effect of injury on total DCX+ cell number (Supplementary Figure 5D) or on DCX+ cell number in the anterior (Supplementary Figure 5E) or posterior (Supplementary Figure 5F) contralateral SGZ.

Thirty-One Dpi (28 Days Post-BrdU Injection), the Number of BrdU+ Cells in the Contralateral SGZ Is Similar Between Sham and LFPI Mice

In the contralateral SGZ of Sham and LFPI mice 31 dpi, there was no effect of injury on total BrdU+ cell number (Supplementary Figure 5G) or on BrdU+ cell number in the anterior (Supplementary Figure 5H) or posterior (Supplementary Figure 5I) contralateral SGZ.

Thirty-One Dpi: Proliferation and Cell Survival Indices in the Ipsilateral and Contralateral DG Non-neurogenic Regions

Thirty-One Dpi, the Number of Ki67+ Proliferating Cells in the Ipsilateral Non-SGZ DG Subregions Are Similar in Sham and LFPI Mice, but the Numbers of Surviving BrdU+ Cells in the Ipsilateral Non-SGZ DG Subregions Are Higher in LFPI vs. Sham Mice

In the ipsilateral DG 31 dpi, there was no effect of injury on Ki67+ cell number in the total hilus, oGCL, or Mol (Figures 7A,G,M) or in the anterior or posterior hilus, oGCL, or Mol (Figures 7B,C,H,I,N,O). However similar to the ipsilateral SGZ 31 dpi, in the ipsilateral DG 31 dpi, there was an effect of injury on BrdU+ cell number in the total hilus, oGCL, and Mol (Figures 7D,J,P) with ~460%, 75%, and 230% more BrdU+ cells, respectively, in LFPI vs Sham mice. When divided into anterior/posterior bins, there was an effect of injury in the anterior and posterior hilus (Figures 7E,F), posterior oGCL (Figure 7L), and anterior and posterior molecular layer (Figures 7Q,R) with 460%, 470%, 85%, 210%, and 260% more BrdU+ cells in these regions in LFPI vs. Sham mice 31 dpi. Together, these data suggest that more BrdU+ cells in other non-SGZ subregions survive out to 31 dpi in LFPI vs. Sham mice.

TABLE 1 | Granule cell layer (GCL) volume in the ipsilateral and contralateral hemispheres, 3, 7, and 31 days post-injury (dpi).

Time point	Ipsilateral GCL volume (mm ³)				Contralateral GCL volume (mm ³)			
	Sham		LFPI		Sham		LFPI	
	Mean	SEM	Mean	SEM	Mean	SEM	Mean	SEM
3 dpi	0.627	0.016	0.582	0.016	0.632	0.021	0.605	0.019
7 dpi	0.658	0.039	0.623	0.033	0.678	0.015	0.659	0.015
31 dpi	0.602	0.020	0.543	0.030	0.591	0.025	0.548	0.017

Mean ipsilateral and contralateral GCL volume values in Sham and LFPI mice at 3 different time points, shown in mm³.

Thirty-One Dpi, the Numbers of Ki67+ Proliferating Cells and BrdU+ Cells in the Contralateral Non-SGZ DG Subregions Are Similar in Sham and LFPI Mice

In the contralateral DG 31 dpi, there was no effect of injury on Ki67+ cell number in the total hilus, oGCL, or Mol (Supplementary Figures 6A,G,M) or in the anterior or posterior hilus, oGCL, or Mol (Supplementary Figures 6B,C,H,I,N,O). Similarly, and in contrast to the greater number of surviving BrdU+ cells in the ipsilateral hemisphere in LFPI vs. Sham mice, in the contralateral DG 31 dpi, there was no effect of injury on BrdU+ cell number in the total hilus, oGCL, or Mol (Supplementary Figures 6D,J,P) or in the anterior or posterior hilus, oGCL, or Mol (Supplementary Figures 6E,F,K,L,Q,R).

DG GCL Volume 3, 7, and 31 Days After Sham or LFPI

Given that in the ipsilateral hemisphere LFPI mice had greater proliferation 3 dpi, more immature/neuroblasts 7 dpi, and more surviving BrdU+ cells 31 dpi relative to Sham mice (Figure 8), it is important to see if these cell number changes influence total volume of the GCL. In fact, assessing GCL volume is critical for interpretation of cell number changes (McDonald and Wojtowicz, 2005; Harburg et al., 2007; Brummelte and Galea, 2010). The results of the Cavalieri Estimator to measure ipsilateral and contralateral GCL volume 3, 7, and 31 dpi are provided in Table 1. In brief, there was no effect of injury

on GCL volume at any time point in either the ipsilateral or contralateral hemisphere. These volume data suggest that the change in neurogenesis is a true change in the underlying process, rather than a matter of scale to match volume changes.

DISCUSSION

In the preclinical TBI literature - even within the minority of studies focused specifically on mild injuries - there is disagreement about if and how mTBI changes the process of DG neurogenesis. Here we utilized a clinically relevant rodent model of mTBI (LFPI), gold-standard neurogenesis markers and quantification approaches, three time points post-injury, and analysis of defined DG subregions to generate a comprehensive picture of how mTBI affects the process of adult hippocampal DG neurogenesis. We report five major findings, which are also summarized in Figure 8. In the ipsilateral hemisphere classical neurogenic DG regions (SGZ/GCL), LFPI leads to (1) a transient increase in proliferating cells 3 dpi; (2) a transient increase in neuroblasts/immature neurons 7 dpi; and (3) sustained survival of BrdU+ cells 31 dpi, all relative to Sham. In ipsilateral hemisphere DG subregions typically considered to be non-neurogenic (hilus, oGCL, molecular layer), LFPI leads to (4) a transient increase in proliferating cells 3 dpi and (5) sustained survival of BrdU+ cells 31 dpi, both relative to Sham. Our ipsilateral data are in line with the large fraction of literature

IPSILATERAL HEMISPHERE												
	3 dpi				7 dpi				31 dpi			
	SGZ	Hilus	oGCL	Mol	SGZ	Hilus	oGCL	Mol	SGZ	Hilus	oGCL	Mol
Ki67	+45%	+135%	+275%	+240%	=	=	=	=	=	=	=	=
DCX	=				+35%				=			
BrdU	=	+130%	=	+160%	=	=	=	=	+45%	+460%	+75%	+230%
CONTRALATERAL HEMISPHERE												
Ki67	=	+65%	+475%	=	=	=	=	=	=	=	=	=
DCX	=								=			
BrdU	=	=	-75%	=	=	=	=	=	=	=	=	=

FIGURE 8 | Summary of neurogenesis changes in LFPI vs. Sham mice at three time points post-injury. Percent change in LFPI vs. Sham number of cells immunoreactive for Ki67, DCX, and BrdU in the ipsilateral (top) and contralateral (bottom) dentate gyrus (DG) subregions 3 dpi (left column), 7 dpi (middle column), and 31 dpi (right column). These summary percentages reflect data presented in Figures 2-7 and Supplementary Figures 1-6. =, not changed vs. Sham. Light-blue shading, increased in LFPI vs. Sham. Rose shading, decreased in LFPI vs. Sham. White, not determined. Light-gray shading, not part of this study. ¹quantified in both SGZ and GCL. Mol, molecular layer. oGCL, outer granule cell layer. SGZ, subgranular zone.

that reports increased DG neurogenesis in other and more severe models of TBI. However, our data in this mTBI model importantly add temporal, stage-specific, and DG subregional resolution to the literature. Below we discuss these findings in the context of the current literature, consider several interpretations of these data, and mention what they mean for efforts to harness the regenerative capacity of adult-generated DG neurons as a treatment for mTBI-induced cognitive changes.

To gain temporal resolution on how mTBI influences the process of DG neurogenesis, we first examined tissue 3 dpi to (a) avoid the immediate mechanical effects of the LFPI, (b) give the brain time to mount a response to the injury, and (c) select a time point frequently represented in the TBI literature. We found more Ki67+ cells in the ipsilateral SGZ 3 dpi, consistent with the idea that there is increased proliferation in the ipsilateral DG neurogenic niche after TBI (Dash et al., 2001; Chirumamilla et al., 2002; Villasana et al., 2015, 2019). Brain injury-induced increased DG proliferation at this short time point may be due to a variety of factors, from proliferation of microglia or astrocytes subsequent to inflammation (Rola et al., 2006; Piao et al., 2013; Chiu et al., 2016; McAteer et al., 2016; Bedi et al., 2018; Krukowski et al., 2018; Wang et al., 2019) or proliferation of neural stem cells and progenitors due to abnormal network activity. Careful readers may have noticed more Ki67+ cells (**Figures 2A–C**) but no change in BrdU+ cell number (**Figures 2G–I**) in LFPI vs. Sham mice 3 dpi (**Figure 8**). This apparent discrepancy between these markers of proliferating cells can be accounted for by their distinct uses: exogenous BrdU is incorporated only by cells in S phase, while endogenous Ki67 is expressed in cells throughout all cell cycle stages. As seen in prior work (Arguello et al., 2008; Lagace et al., 2010; Farioli-Vecchioli et al., 2012), this disconnect between these markers of proliferation may reflect a change in the number of cycling cells, or even the length of the cell cycle. Future work specifically assessing how mTBI changes SGZ cell cycle kinetics is warranted to address these possibilities.

The next time point, 7 dpi, was also selected due to it being consistently examined for TBI-induced changes in electrophysiology and behavior (Santhakumar et al., 2000, 2001; Schurman et al., 2017; Zhang et al., 2018). Indeed, the same LFPI parameters used here have been shown to result in DG hyperexcitability and deficits in DG-based cognition 7 dpi (Smith et al., 2012; Folweiler et al., 2018; Paterno et al., 2018), implying that hippocampal circuitry is disrupted in this mTBI model 7 dpi. An additional reason for choosing 7 dpi is that it allowed comparison to the progression of neurogenesis indices relative to 3 dpi. Based on the TBI-induced DG hyperactivity 7 dpi and the well-known ability of neuronal activity to stimulate neurogenesis (Kempermann, 2015; Kempermann et al., 2015; Kárádóttir and Kuo, 2018), we expected to see more DCX+ cells 7 dpi, which we did (**Figure 8**). One interpretation of the increased DCX+ cells 7 dpi in the ipsilateral SGZ/GCL in LFPI vs. Sham mice is that at least some of the proliferating cells in the SGZ seen at 3 dpi express markers of immature neurons 4 days later at 7 dpi.

Previous work suggests that cells in the immature neuron stage at the time of injury (cells ‘born’ before the injury) are vulnerable to injury-induced cell death (Gao et al., 2008, 2009; Zhou et al., 2012; Hood et al., 2018). Our study did not

directly assess the susceptibility of existing immature neurons to mTBI, as we were focused on the influence of mTBI on the process of neurogenesis after the injury. However, in this study, two pieces of our data suggest existing immature neurons are not susceptible to mild LFPI-induced cell death. First, if immature DCX+ cells were vulnerable to injury-induced death, we might expect to see a fewer DCX+ cells 3 dpi in the ipsilateral SGZ/GCL LFPI vs. Sham mice, as this population in part reflects cells born before the injury. However, we find DCX+ cell numbers are similar between Sham and LFPI mice 3 dpi. Second, if there was significant death of the DCX+ population after injury, we might expect a smaller GCL at the short-term time point; instead, we see similar DG GCL volume 3 dpi in Sham and LFPI mice. While these data suggest there is no gross loss of immature neurons due to the injury, future studies could directly address this by giving a BrdU injection prior to injury to label a cohort of cells born before the TBI, or by examining time points after the injury even earlier than 3 dpi.

In some models of injury, DCX+ cells have been reported outside the canonical DG neurogenic regions (the SGZ and inner GCL; Ibrahim et al., 2016; Shapiro, 2017). In our work here with an mTBI model, DCX+ cells in the oGCL were rare, thus we combined DCX+ cell counts in the inner and oGCL and SGZ. In addition, DCX+ cells in the hilus and molecular layer had ambiguous/faint staining, preventing reliable quantification of DCX+ cells in these non-canonical neurogenic DG regions. While this suggests our mTBI model leads to minimal DCX+ cells present outside of the SGZ and GCL, it is also possible that a more sensitive approach - such as a transgenic DCX+ reporter mouse - or distinct study design - such as labeling mitotic cells prior to injury - may reveal LFPI-induced DCX+ cells outside of these canonical DG neurogenic regions.

The final 31 dpi time point matches with evidence that the ipsilateral DG remains hyperexcitable 30 dpi (Tran et al., 2006) as well as the ~4 weeks it takes for adult-born granule cells to integrate fully into hippocampal circuitry (Brown et al., 2003; Gu et al., 2012). The BrdU injected 3 dpi intercalates into DNA of dividing cells such that staining for BrdU at 3 dpi will reveal the progeny of the initially labeled cells that survived to 31 dpi. Here we report more BrdU+ cells in the ipsilateral SGZ 31 dpi in LFPI vs. Sham mice. As LFPI and Sham mice had the same number of BrdU+ cells 3 dpi (**Figures 2G–I**) and 7 dpi (**Figures 4G–I**), this emergence of more BrdU+ cells in LFPI vs. Sham SGZ 31 dpi combined with the overall fewer BrdU+ cells in 31 vs. 3 dpi tissue (**Figures 6G–I**) suggests an effect of survival (**Figure 8**). In other words, the rate of survival of BrdU+ cells in LFPI mice was higher (or the rate of death was lower) than the rate of BrdU+ in Sham mice. While the mechanisms mediating this difference are beyond the scope of this study, it is intriguing to consider if the TBI-induced hyperactivity reported 30 dpi (Tran et al., 2006) is responsible for this LFPI-induced survival, particularly given the well-described “activity-dependence” of adult-generated neurons (Deisseroth et al., 2004; Ma et al., 2009; Kárádóttir and Kuo, 2018).

One caveat when discussing BrdU+ cells in the intermediate (7 dpi) and long-term (31 dpi) groups is that the DG subregion may influence the data interpretation. In the DG of naive adult male mice, BrdU has an *in vivo* half-life of 15 minutes (Mandyam et al., 2007), and thus BrdU labels cells that are in S-phase at the time of injection. In the SGZ, where the cell cycle is known to be 12 hours (Mandyam et al., 2007), we believe BrdU+ cells 7 and 31 dpi are post-mitotic, not cells that are still dividing. We favor this interpretation in the SGZ, as more than a few cell cycles would dilute the BrdU and make cells less likely to be detected via IHC (Dayer et al., 2003). Further supporting a post-mitotic state for SGZ BrdU+ cells 7 and 31 dpi is that our LFPI mice have more Ki67+ SGZ cells vs. Sham mice at 3 dpi, but LFPI and Sham Ki67+ SGZ cell numbers are similar at 7 and 31 dpi. Beyond being post-mitotic, we also suspect BrdU+ SGZ cells 31 dpi are mature granule cell neurons, but this speculation merits more discussion (see the first ‘future direction’ below). Outside of the SGZ, it is more likely that BrdU injection 3 dpi labels proliferating cells whose progeny become non-neuronal cells. Certainly, reactive gliosis is evident in many brain regions in other and more severe TBI models (Acosta et al., 2013; Newell et al., 2019; Caplan et al., 2020). The spatiotemporal extent and severity of reactive astro- and micro-gliosis in DG subregions in this mild LFPI model is less well-studied, although there is reactive astrocytosis in the ipsilateral hippocampus 7 dpi (Smith et al., 2015). Therefore, it is possible (and even likely) that dividing glia or other brain cells take up BrdU (from the BrdU injection administered 3 dpi) and persist in the hilus, oGCL, and molecular layer, DG subregions which have distinct cell cycle kinetics from the SGZ (Mandyam et al., 2007), and thus whose progeny may still be proliferating 7 and 31 dpi. If these progeny of hilus, oGCL, and molecular layer cells do become post-mitotic, it is also possible their non-neuronal post-mitotic progeny survive to 7 and 31 dpi. While these are reasonable speculations, these possible DG subregion-dependent state and fate outcomes warrant testing with cell cycle markers in both Sham and LFPI tissue, and multiple time points. Minimally, though, our data suggest the importance of considering the dynamics and DG subregion-dependent effects of injury-induced neurogenesis.

While we report LFPI leads to transient, sequential changes in proliferating cells, neuroblasts/immature neurons, and surviving cells, we find no LFPI-induced change in DG granule cell layer volume (Table 1). Volume is an important consideration since more new cells may be compensating for TBI-induced cell loss caused by the injury. However, our data suggest there is no decrease in the size of the GCL, and therefore no major tissue loss, raising the possibility of overcompensation by the brain. Additionally, many papers examining neurogenesis after TBI report neurogenic cell counts in terms of density, not in terms of stereologically determined cell number. While density is a useful metric, reporting both GCL volume and cell counts allows for comparison with those studies while preserving data resolution (increased density of new neurons could be from either increased number of cells or a decrease in volume). Therefore, our data demonstrating more neurogenesis in the

absence of increased GCL volume reflects a true increase in the neurogenic rate.

Our findings raise several important future directions. First, it will be important to definitively determine how mTBI influences the fate and integration of adult-generated DG granule cells into DG circuitry. As for the fate of these cells, there are several reasons we interpret the LFPI-induced increase in BrdU+ SGZ cells 31 dpi as reflecting increased survival specifically of adult-born DG granule cells. This interpretation is supported by the size, shape, and location of the BrdU+ cells. The BrdU+ nuclei are the right size (~10um) to be neuronal nuclei of DG granule neurons. The cell bodies of the BrdU+ nuclei are circular, suggestive of neurons (or at least not suggestive of reactive astrocytes or other glia), and they are in the SGZ and inner GCL where most adult-generated neurons end up (Kempermann et al., 2003). While it is possible that some of the BrdU+ cells 31 dpi outside of the neurogenic SGZ/GCL are glia or other brain cells, most astrocytes and microglia reside in the hilus and molecular layer and only sparsely populate the GCL. Nevertheless, conclusive determination of the neuronal fate of BrdU+ SGZ cells 31 dpi will require phenotypic analysis of BrdU+ SGZ cells 31 dpi with a neuronal marker and/or electrophysiological characterization. Second, as other models of TBI and seizure models result in aberrant migration of adult-born DG neurons (Dashtipour et al., 2003; Emery et al., 2005; Shapiro et al., 2008, 2011; Murphy et al., 2012; Ibrahim et al., 2016; Ratliff et al., 2020), future work could assess whether the greater number of BrdU+ cells in DG subregions adjacent to the SGZ (hilus and oGCL) means this may also be occurring in our mTBI model. In our study, DCX+ staining in non-neurogenic regions was ambiguous, but future work using transgenic or viral-mediated visualization of DCX+ cells or the neuronal phenotyping mentioned above would be useful in this regard (van Praag et al., 2002; Laplagne et al., 2006; Wood et al., 2011; Kathner-Schaffert et al., 2019; Cole et al., 2020; Tensaouti et al., 2020). Third, it will be important to assess if our mTBI model changes the dendritic morphology of the adult-born DG granule cells as has been reported in other and more severe TBI models (Folkerts et al., 1998; Gao et al., 2011; Villasana et al., 2015; Ibrahim et al., 2016). In this mTBI model, there were no injury-induced gross visual differences in DCX+ process length, thickness, or angle. However, our stained DG tissue was marked by a high density of immature neuron processes, typical of DCX+ staining in young adult mice (Wu and Hen, 2014; Villasana et al., 2019), and this prevented performing a rigorous quantitative analysis of dendritic morphology. Future studies could more carefully address the impact of mTBI on dendritic morphology using alternative methods (i.e., fluorescent retroviral labeling) to more sparsely label new DG neurons, allowing for high-resolution analysis of newborn cell dendritic morphology.

A final future direction will be to clarify the question of functional significance of the injury-induced transient surge of proliferating cells, immature neurons, and surviving cells shown here. Certainly, in uninjured animals, DG neurogenesis is critical for cognitive function (Clelland et al., 2009; Sahay et al., 2011). After injury, the prevailing idea is that increased neurogenesis

represents an attempt by the brain to repair itself, and thus it aids functional recovery (Blaiss et al., 2011; Sun et al., 2015). However, preclinical work in seizures (Cho et al., 2015) and TBI (Neuberger et al., 2017) have questioned the assumption that more new neurons are always beneficial, and underscore that the timing and methods of manipulating new DG neurons may influence the outcome of such studies. Because adult-born neurons are exquisitely sensitive to external cues (Ming and Song, 2005; Aimone et al., 2014; Bond et al., 2015; Kempermann et al., 2015; Catavero et al., 2018), the pathological environment of a post-injury dentate has the potential to influence newborn neuron development in a maladaptive manner. Therefore, the question of reparative potential of injury-induced neurogenesis needs to be explicitly tested in a less invasive manner than ablation of new neurons; chemogenetic or optogenetic manipulation of injury-induced neurons would allow more accurate inquiry into how injury-induced neurons influence hippocampal function.

Together, these data suggest this model of mTBI induces transient, sequential increases in ipsilateral SGZ/GCL proliferating cells, immature neurons, and surviving cells which we interpret as a transient increase in mTBI-induced neurogenesis. Our work in this mTBI model is in line with other and more severe models of TBI, where the large fraction of literature shows injury-induced stimulation of DG neurogenesis. As our data in this mTBI model provide temporal, subregional, and neurogenesis-stage resolution, these data are important to consider in regard to the functional importance of TBI-induced neurogenesis and future work assessing the potential of replacing and/or repairing DG neurons in the brain after TBI. Indeed, the transient nature of the injury-induced increase in neurogenesis provides temporal guidance about a discrete window for targeting injury-induced adult-born neurons. Because DCX+ cells are increased 7 dpi, but not 3 or 31 dpi, it is the neurons born during that intermediate timeframe that have the most potential to disrupt the circuit. This is good news for future work attempting to target these cells for chemogenetic or optogenetic targeting, as it narrows down the temporal window and population subset for targeting. We hope future work will consider the “age” of the cells, time post-injury, and anatomical location and integration of the cells, as these parameters may prove useful to achieve therapeutic potential of any intervention strategy.

DATA AVAILABILITY STATEMENT

The raw data supporting the conclusions of this article will be made available by the authors, without undue reservation.

REFERENCES

Acosta, S. A., Tajiri, N., Shinozuka, K., Ishikawa, H., Grimmig, B., Diamond, D. M., et al. (2013). Long-term upregulation of inflammation and suppression of cell proliferation in the brain of adult rats exposed to traumatic brain injury using the controlled cortical impact model. *PLoS One* 8:e53376. doi: 10.1371/journal.pone.0053376

ETHICS STATEMENT

The animal study was reviewed and approved by the IACUC – Children’s Hospital of Philadelphia.

AUTHOR CONTRIBUTIONS

AE, AC, LC, and SY did the conceptualization and carried out the experimental design. LC and HM performed the methodology. LC and NA validated the data. LC, NA, RP, and PK carried out the formal analysis. AE, HM, LC, and SY investigated the data. AE and AC carried out the resources and funding acquisition. AE and LC performed the data curation, wrote, reviewed and edited the original draft of the manuscript, and carried out the project administration. LC visualized the data. AE, AC, SY, and LC supervised the data.

FUNDING

Funding for this work was provided by grants to AC (R37HD059288) and AE (DA023555, NNX15AE09G, 80NSSC17K0060, MH117628, and NS007413, PI: MB Robinson). LC was supported by NIH T32-GM07517 (PI: JI Gold). SY was supported by Penn’s McCabe Pilot Award, a Penn Undergraduate Research Foundation Award, and a NARSAD Young Investigator Award from the Brain and Behavior Research Foundation. NA was supported by Penn’s Center for Undergraduate Research and Fellowships (CURF) program. PK was supported by Penn’s Undergraduate Research Mentoring Program (PURM). RP was supported by CHOP Research Institute Summer Scholars Program (CRISSP).

ACKNOWLEDGMENTS

We thank Giulia Zanni and Kait Folweiler for helpful discussion about initial experiment design and Danielle Barber for discussions about the role of microglia in the reported results. We also thank Ryan Reynolds for his initial graphic design that inspired **Figures 1D–F**.

SUPPLEMENTARY MATERIAL

The Supplementary Material for this article can be found online at: <https://www.frontiersin.org/articles/10.3389/fnins.2020.612749/full#supplementary-material>

Aertker, B. M., Bedi, S., and Cox, C. S. Jr. (2016). Strategies for CNS repair following TBI. *Exp. Neurol.* 275(Pt 3), 411–426. doi: 10.1016/j.expneurol.2015.01.008

Aimone, J. B., Li, Y., Lee, S. W., Clemenson, G. D., Deng, W., and Gage, F. H. (2014). Regulation and function of adult neurogenesis: from genes to cognition. *Physiol. Rev.* 94, 991–1026. doi: 10.1152/physrev.00004.2014

- Aleem, M., Goswami, N., Kumar, M., and Manda, K. (2020). Low-pressure fluid percussion minimally adds to the sham craniectomy-induced neurobehavioral changes: Implication for experimental traumatic brain injury model. *Exp. Neurol.* 329:113290. doi: 10.1016/j.expneurol.2020.113290
- Arguello, A. A., Harburg, G. C., Schonborn, J. R., Mandyam, C. D., Yamaguchi, M., and Eisch, A. J. (2008). Time course of morphine's effects on adult hippocampal subgranular zone reveals preferential inhibition of cells in S phase of the cell cycle and a subpopulation of immature neurons. *Neuroscience* 157, 70–79. doi: 10.1016/j.neuroscience.2008.08.064
- Avendaño, C., and Cowan, W. M. (1979). A study of glial cell proliferation in the molecular layer of the dentate gyrus of the rat following interruption of the ventral hippocampal commissure. *Anat. Embryol.* 157, 347–366. doi: 10.1007/bf00304998
- Basler, L., Gerdes, S., Wolfer, D. P., and Slomianka, L. (2017). Sampling the mouse hippocampal dentate Gyrus. *Front. Neuroanat.* 11:123. doi: 10.3389/fnana.2017.00123
- Bedi, S. S., Aertker, B. M., Liao, G. P., Caplan, H. W., Bhattarai, D., Mandy, F., et al. (2018). Therapeutic time window of multipotent adult progenitor therapy after traumatic brain injury. *J. Neuroinflamm.* 15:84.
- Bielefeld, P., Durá, I., Danielewicz, J., Lucassen, P. J., Baekelandt, V., Abrous, D. N., et al. (2019). Insult-induced aberrant hippocampal neurogenesis: Functional consequences and possible therapeutic strategies. *Behav. Brain Res.* 372:112032. doi: 10.1016/j.bbr.2019.112032
- Blais, C. A., Yu, T.-S., Zhang, G., Chen, J., Dimchev, G., Parada, L. F., et al. (2011). Temporally specified genetic ablation of neurogenesis impairs cognitive recovery after traumatic brain injury. *J. Neurosci.* 31, 4906–4916. doi: 10.1523/jneurosci.5265-10.2011
- Blümcke, I., Schewe, J.-C., Normann, S., Brüstle, O., Schramm, J., Elger, C. E., et al. (2001). Increase of nestin-immunoreactive neural precursor cells in the dentate gyrus of pediatric patients with early-onset temporal lobe epilepsy. *Hippocampus* 11, 311–321. doi: 10.1002/hipo.1045
- Bond, A. M., Ming, G.-L., and Song, H. (2015). Adult mammalian neural stem cells and neurogenesis: five decades later. *Cell Stem Cell* 17, 385–395. doi: 10.1016/j.stem.2015.09.003
- Brady, R. D., Casillas-Espinosa, P. M., Agoston, D. V., Bertram, E. H., Kamnaksh, A., Semple, B. D., et al. (2018). Modelling traumatic brain injury and posttraumatic epilepsy in rodents. *Neurobiol. Dis.* 123, 8–19. doi: 10.1016/j.nbd.2018.08.007
- Brown, D. C., and Gatter, K. C. (2002). Ki67 protein: the immaculate deception? *Histopathology* 40, 2–11. doi: 10.1046/j.1365-2559.2002.01343.x
- Brown, J. P., Couillard-Després, S., Cooper-Kuhn, C. M., Winkler, J., Aigner, L., and Kuhn, H. G. (2003). Transient expression of doublecortin during adult neurogenesis. *J. Comp. Neurol.* 467, 1–10. doi: 10.1002/cne.10874
- Brummelte, S., and Galea, L. A. M. (2010). Chronic high corticosterone reduces neurogenesis in the dentate gyrus of adult male and female rats. *Neuroscience* 168, 680–690. doi: 10.1016/j.neuroscience.2010.04.023
- Bye, N., Carron, S., Han, X., Agyapomaa, D., Ng, S. Y., Yan, E., et al. (2011). Neurogenesis and glial proliferation are stimulated following diffuse traumatic brain injury in adult rats. *J. Neurosci. Res.* 89, 986–1000. doi: 10.1002/jnr.22635
- Cameron, H. A., and McKay, R. D. (2001). Adult neurogenesis produces a large pool of new granule cells in the dentate gyrus. *J. Comp. Neurol.* 435, 406–417. doi: 10.1002/cne.1040
- Caplan, H. W., Cardenas, F., Gudenkauf, F., Zelnick, P., Xue, H., Cox, C. S., et al. (2020). Spatiotemporal distribution of microglia after traumatic brain injury in male mice. *ASN Neuro* 12:1759091420911770.
- Carlson, S. W., and Saatman, K. E. (2018). Central infusion of insulin-like growth factor-1 increases hippocampal neurogenesis and improves neurobehavioral function after traumatic brain injury. *J. Neurotrauma* 35, 1467–1480. doi: 10.1089/neu.2017.5374
- Catavero, C., Bao, H., and Song, J. (2018). Neural mechanisms underlying GABAergic regulation of adult hippocampal neurogenesis. *Cell Tissue Res.* 371, 33–46. doi: 10.1007/s00441-017-2668-y
- Chirumamilla, S., Sun, D., Bullock, M. R., and Colello, R. J. (2002). Traumatic brain injury induced cell proliferation in the adult mammalian central nervous system. *J. Neurotrauma* 19, 693–703. doi: 10.1089/08977150260139084
- Chiu, C.-C., Liao, Y.-E., Yang, L.-Y., Wang, J.-Y., Tweedie, D., Karnati, H. K., et al. (2016). Neuroinflammation in animal models of traumatic brain injury. *J. Neurosci. Methods* 272, 38–49.
- Cho, K.-O., Lybrand, Z. R., Ito, N., Brulet, R., Tafacory, F., Zhang, L., et al. (2015). Aberrant hippocampal neurogenesis contributes to epilepsy and associated cognitive decline. *Nat. Commun.* 6:6606.
- Clelland, C. D., Choi, M., Romberg, C., Clemenson, G. D. Jr., Fragniere, A., Tyers, P., et al. (2009). A functional role for adult hippocampal neurogenesis in spatial pattern separation. *Science* 325, 210–213. doi: 10.1126/science.1173215
- Cole, J. D., Espinueva, D., Seib, D. R., Ash, A. M., Cooke, M. B., Cahill, S. P., et al. (2020). Adult-born hippocampal neurons undergo extended development and are morphologically distinct from neonatally-born neurons Prolonged development of adult-born neurons. *J. Neurosci.* 40, 5740–5756. doi: 10.1523/JNEUROSCI.1665-19.2020
- Couillard-Despres, S., Winner, B., Schaubeck, S., Aigner, R., Vroemen, M., Weidner, N., et al. (2005). Doublecortin expression levels in adult brain reflect neurogenesis. *Eur. J. Neurosci.* 21, 1–14. doi: 10.1111/j.1460-9568.2004.03813.x
- Daneshvar, D. H., Riley, D. O., Nowinski, C. J., McKee, A. C., Stern, R. A., and Cantu, R. C. (2011). Long-term consequences: effects on normal development profile after concussion. *Phys. Med. Rehabil. Clin. N. Am.* 22, 683–700. doi: 10.1016/j.pmr.2011.08.009
- Dash, P. K., Mach, S. A., and Moore, A. N. (2001). Enhanced neurogenesis in the rodent hippocampus following traumatic brain injury. *J. Neurosci. Res.* 63, 313–319. doi: 10.1002/1097-4547(20010215)63:4<313::aid-jnr1025>3.0.co;2-4
- Dashtipour, K., Wong, A. M., Obenaus, A., Spigelman, I., and Ribak, C. E. (2003). Temporal profile of hilar basal dendrite formation on dentate granule cells after status epilepticus. *Epilepsy Res.* 54, 141–151. doi: 10.1016/s0920-1211(03)00082-2
- Dayer, A. G., Ford, A. A., Cleaver, K. M., Yassaee, M., and Cameron, H. A. (2003). Short-term and long-term survival of new neurons in the rat dentate gyrus. *J. Comp. Neurol.* 460, 563–572. doi: 10.1002/cne.10675
- DeCarolis, N. A., Rivera, P. D., Ahn, F., Amaral, W. Z., LeBlanc, J. A., Malhotra, S., et al. (2014). 56Fe particle exposure results in a long-lasting increase in a cellular index of genomic instability and transiently suppresses adult hippocampal neurogenesis in vivo. *Life Sci. Space Res.* 2, 70–79. doi: 10.1016/j.lssr.2014.06.004
- Deisseroth, K., Singla, S., Toda, H., Monje, M., Palmer, T. D., and Malenka, R. C. (2004). Excitation-neurogenesis coupling in adult neural stem/progenitor cells. *Neuron* 42, 535–552. doi: 10.1016/s0896-6273(04)00266-1
- Dixon, C. E., Lyeth, B. G., Povlishock, J. T., Findling, R. L., Hamm, R. J., Marmarou, A., et al. (1987). A fluid percussion model of experimental brain injury in the rat. *J. Neurosurg.* 67, 110–119.
- Dragunow, M., de Castro, D., and Faull, R. L. (1990). Induction of Fos in glia-like cells after focal brain injury but not during wallerian degeneration. *Brain Res.* 527, 41–54. doi: 10.1016/0006-8993(90)91058-o
- Du, X., Zhang, H., and Parent, J. M. (2017). Rabies tracing of birthdated dentate granule cells in rat temporal lobe epilepsy. *Ann. Neurol.* 81, 790–803. doi: 10.1002/ana.24946
- Eakin, K., and Miller, J. P. (2012). Mild traumatic brain injury is associated with impaired hippocampal spatiotemporal representation in the absence of histological changes. *J. Neurotrauma* 29, 1180–1187. doi: 10.1089/neu.2011.2192
- Emery, D. L., Fulp, C. T., Saatman, K. E., Schütz, C., Neugebauer, E., and McIntosh, T. K. (2005). Newly born granule cells in the dentate gyrus rapidly extend axons into the hippocampal CA3 region following experimental brain injury. *J. Neurotrauma* 22, 978–988. doi: 10.1089/neu.2005.22.978
- Farioli-Vecchioli, S., Micheli, L., Saraulli, D., Ceccarelli, M., Cannas, S., Scardigli, R., et al. (2012). Btg1 is required to maintain the pool of stem and progenitor cells of the dentate gyrus and subventricular zone. *Front. Neurosci.* 6:124. doi: 10.3389/fnins.2012.00124
- Faul, M., Xu, L., Wald, M. M., and Coronado, V. G. (2010). *Traumatic Brain Injury in the United States: Emergency Department Visits, Hospitalizations, and Deaths*. Atlanta: Centers for Disease Control and Prevention.
- Folkerts, M. M., Berman, R. F., Muizelaar, J. P., and Rafols, J. A. (1998). Disruption of MAP-2 immunostaining in rat hippocampus after traumatic brain injury. *J. Neurotrauma* 15, 349–363. doi: 10.1089/neu.1998.15.349

- Folweiler, K., Samuel, S., Metheny, H., and Cohen, A. S. (2018). Diminished dentate gyrus filtering of cortical input leads to enhanced area CA3 excitability after mild traumatic brain injury. *J. Neurotrauma* 35, 1304–1317. doi: 10.1089/neu.2017.5350
- Francis, F., Koulakoff, A., Boucher, D., Chafey, P., Schaar, B., Vinet, M. C., et al. (1999). Doublecortin is a developmentally regulated, microtubule-associated protein expressed in migrating and differentiating neurons. *Neuron* 23, 247–256. doi: 10.1016/s0896-6273(00)80777-1
- Gao, X., Deng, P., Xu, Z. C., and Chen, J. (2011). Moderate traumatic brain injury causes acute dendritic and synaptic degeneration in the hippocampal dentate gyrus. *PLoS One* 6:e24566. doi: 10.1371/journal.pone.0024566
- Gao, X., Deng-Bryant, Y., Cho, W., Carrico, K. M., Hall, E. D., and Chen, J. (2008). Selective death of newborn neurons in hippocampal dentate gyrus following moderate experimental traumatic brain injury. *J. Neurosci. Res.* 86, 2258–2270. doi: 10.1002/jnr.21677
- Gao, X., Enikolopov, G., and Chen, J. (2009). Moderate traumatic brain injury promotes proliferation of quiescent neural progenitors in the adult hippocampus. *Exp. Neurol.* 219, 516–523. doi: 10.1016/j.expneurol.2009.07.007
- García-Martínez, Y., Sánchez-Huerta, K. B., and Pacheco-Rosado, J. (2020). Quantitative characterization of proliferative cells subpopulations in the hilus of the hippocampus of adult Wistar rats: an integrative study. *J. Mol. Histol.* 51, 437–453. doi: 10.1007/s10735-020-09895-4
- Gilley, J. A., and Kernie, S. G. (2011). Excitatory amino acid transporter 2 and excitatory amino acid transporter 1 negatively regulate calcium-dependent proliferation of hippocampal neural progenitor cells and are persistently upregulated after injury. *Eur. J. Neurosci.* 34, 1712–1723. doi: 10.1111/j.1460-9568.2011.07888.x
- Gu, Y., Arruda-Carvalho, M., Wang, J., Janoschka, S. R., Josselyn, S. A., Frankland, P. W., et al. (2012). Optical controlling reveals time-dependent roles for adult-born dentate granule cells. *Nat. Neurosci.* 15, 1700–1706. doi: 10.1038/nn.3260
- Gundersen, H. J., Bendtsen, T. F., Korbo, L., Marcussen, N., Møller, A., Nielsen, K., et al. (1988). Some new, simple and efficient stereological methods and their use in pathological research and diagnosis. *APMIS* 96, 379–394. doi: 10.1111/j.1699-0463.1988.tb05320.x
- Gundersen, H. J. G., and Jensen, E. B. (1987). The efficiency of systematic sampling in stereology and its prediction*. *J. Microsc.* 147, 229–263. doi: 10.1111/j.1365-2818.1987.tb02837.x
- Hailer, N. P., Grampp, A., and Nitsch, R. (1999). Proliferation of microglia and astrocytes in the dentate gyrus following entorhinal cortex lesion: a quantitative bromodeoxyuridine-labelling study. *Eur. J. Neurosci.* 11, 3359–3364. doi: 10.1046/j.1460-9568.1999.00808.x
- Harburg, G. C., Hall, F. S., Harrist, A. V., Sora, I., Uhl, G. R., and Eisch, A. J. (2007). Knockout of the mu opioid receptor enhances the survival of adult-generated hippocampal granule cell neurons. *Neuroscience* 144, 77–87. doi: 10.1016/j.neuroscience.2006.09.018
- Hood, K. N., Zhao, J., Redell, J. B., Hylin, M. J., Harris, B., Perez, A., et al. (2018). Endoplasmic reticulum stress contributes to the loss of newborn hippocampal neurons after traumatic brain injury. *J. Neurosci.* 38, 2372–2384. doi: 10.1523/JNEUROSCI.1756-17.2018
- Hsu, D. (2007). “The dentate gyrus as a filter or gate: a look back and a look ahead,” in *Progress in Brain Research*, ed. H. E. Scharfman (Amsterdam: Elsevier), 601–613. doi: 10.1016/s0079-6123(07)63032-5
- Ibrahim, S., Hu, W., Wang, X., Gao, X., He, C., and Chen, J. (2016). Traumatic brain injury causes aberrant migration of adult-born neurons in the hippocampus. *Sci. Rep.* 6:21793.
- Ikrar, T., Guo, N., He, K., Besnard, A., Levinson, S., Hill, A., et al. (2013). Adult neurogenesis modifies excitability of the dentate gyrus. *Front. Neural Circuits* 7:204. doi: 10.3389/fncir.2013.00204
- Káradóttir, R. T., and Kuo, C. T. (2018). Neuronal activity-dependent control of postnatal neurogenesis and gliogenesis. *Annu. Rev. Neurosci.* 41, 139–161. doi: 10.1146/annurev-neuro-072116-031054
- Kathner-Schaffert, C., Karapetow, L., Günther, M., Rudolph, M., Dahab, M., Baum, E., et al. (2019). Early stroke induces long-term impairment of adult neurogenesis accompanied by hippocampal-mediated cognitive decline. *Cells* 8:1654. doi: 10.3390/cells8121654
- Katz, D. I., Cohen, S. I., and Alexander, M. P. (2015). Mild traumatic brain injury. *Handb. Clin. Neurol.* 127, 131–156.
- Kempermann, G. (2015). Activity dependency and aging in the regulation of adult neurogenesis. *Cold Spring Harb. Perspect. Biol.* 7:a018929. doi: 10.1101/cshperspect.a018929
- Kempermann, G., Gast, D., Kronenberg, G., Yamaguchi, M., and Gage, F. H. (2003). Early determination and long-term persistence of adult-generated new neurons in the hippocampus of mice. *Development* 130, 391–399. doi: 10.1242/dev.00203
- Kempermann, G., Song, H., and Gage, F. H. (2015). Neurogenesis in the adult hippocampus. *Cold Spring Harb. Perspect. Biol.* 7:a018812.
- Kernie, S. G., Erwin, T. M., and Parada, L. F. (2001). Brain remodeling due to neuronal and astrocytic proliferation after controlled cortical injury in mice. *J. Neurosci. Res.* 66, 317–326. doi: 10.1002/jnr.10013
- Kezele, T. G., Jakovac, H., Turkoviae, K., Fužinac-Smojver, A., and Ćurko-Cofek, B. (2017). Adult neurogenesis – accent on subgranular and subventricular zone in mammals. *Med. Fluminensis* 53, 136–146. doi: 10.21860/medflum2017_179749
- Krukowski, K., Chou, A., Feng, X., Tiret, B., Paladini, M.-S., Riparip, L.-K., et al. (2018). Traumatic brain injury in aged mice induces chronic microglia activation, synapse loss, and complement-dependent memory deficits. *Int. J. Mol. Sci.* 19:3753. doi: 10.3390/ijms19123753
- La Rosa, C., Ghibaudi, M., and Bonfanti, L. (2019). Newly generated and non-newly generated “immature” neurons in the mammalian brain: a possible reservoir of young cells to prevent brain aging and disease? *J. Clin. Med. Res.* 8:685. doi: 10.3390/jcm8050685
- Lacefield, C. O., Itskov, V., Reardon, T., Hen, R., and Gordon, J. A. (2012). Effects of adult-generated granule cells on coordinated network activity in the dentate gyrus. *Hippocampus* 22, 106–116. doi: 10.1002/hipo.20860
- Lagace, D. C., Donovan, M. H., DeCarolis, N. A., Farnbauch, L. A., Malhotra, S., Berton, O., et al. (2010). Adult hippocampal neurogenesis is functionally important for stress-induced social avoidance. *Proc. Natl. Acad. Sci. U.S.A.* 107, 4436–4441. doi: 10.1073/pnas.0910072107
- Laplagne, D. A., Soledad Espósito, M., Piatti, V. C., Morgenstern, N. A., Zhao, C., van Praag, H., et al. (2006). Functional Convergence of Neurons Generated in the Developing and Adult Hippocampus. *PLoS Biol.* 4:e409. doi: 10.1371/journal.pbio.0040409
- Levone, B. R., Codagnone, M. G., Moloney, G. M., Nolan, Y. M., Cryan, J. F., and O’Leary, O. F. (2020). Adult-born neurons from the dorsal, intermediate, and ventral regions of the longitudinal axis of the hippocampus exhibit differential sensitivity to glucocorticoids. *Mol. Psychiatry* doi: 10.1038/s41380-020-0848-8 [Epub ahead of print].
- Lippert-Grüner, M., Kuchta, J., Hellmich, M., and Klug, N. (2006). Neurobehavioural deficits after severe traumatic brain injury (TBI). *Brain Inj.* 20, 569–574. doi: 10.1080/02699050600664467
- Littlejohn, E. L., Scott, D., and Saatman, K. E. (2020). Insulin-like growth factor-1 overexpression increases long-term survival of posttrauma-born hippocampal neurons while inhibiting ectopic migration following traumatic brain injury. *Acta Neuropathol. Commun.* 8:46.
- Lyeth, B. G., Jenkins, L. W., Hamm, R. J., Dixon, C. E., Phillips, L. L., Clifton, G. L., et al. (1990). Prolonged memory impairment in the absence of hippocampal cell death following traumatic brain injury in the rat. *Brain Res.* 526, 249–258. doi: 10.1016/0006-8993(90)91229-a
- Ma, D. K., Kim, W. R., Ming, G.-L., and Song, H. (2009). Activity-dependent extrinsic regulation of adult olfactory bulb and hippocampal neurogenesis. *Ann. N. Y. Acad. Sci.* 1170, 664–673. doi: 10.1111/j.1749-6632.2009.04373.x
- Mandyam, C. D., Harburg, G. C., and Eisch, A. J. (2007). Determination of key aspects of precursor cell proliferation, cell cycle length and kinetics in the adult mouse subgranular zone. *Neuroscience* 146, 108–122. doi: 10.1016/j.neuroscience.2006.12.064
- McAteer, K. M., Corrigan, F., Thornton, E., Turner, R. J., and Vink, R. (2016). Short and long term behavioral and pathological changes in a novel rodent model of repetitive mild traumatic brain injury. *PLoS One* 11:e0160220. doi: 10.1371/journal.pone.0160220
- McDonald, H. Y., and Wojtowicz, J. M. (2005). Dynamics of neurogenesis in the dentate gyrus of adult rats. *Neurosci. Lett.* 385, 70–75. doi: 10.1016/j.neulet.2005.05.022

- Ming, G.-L., and Song, H. (2005). Adult neurogenesis in the mammalian central nervous system. *Annu. Rev. Neurosci.* 28, 223–250. doi: 10.1146/annurev.neuro.28.051804.101459
- Murphy, B. L., Hofacer, R. D., Faulkner, C. N., Loepke, A. W., and Danzer, S. C. (2012). Abnormalities of granule cell dendritic structure are a prominent feature of the intrahippocampal kainic acid model of epilepsy despite reduced postinjury neurogenesis. *Epilepsia* 53, 908–921. doi: 10.1111/j.1528-1167.2012.03463.x
- Nacher, J., Crespo, C., and McEwen, B. S. (2001). Doublecortin expression in the adult rat telencephalon. *Eur. J. Neurosci.* 14, 629–644. doi: 10.1046/j.0953-816x.2001.01683.x
- Nakashiba, T., Cushman, J. D., Pelkey, K. A., Renaudineau, S., Buhl, D. L., McHugh, T. J., et al. (2012). Young dentate granule cells mediate pattern separation, whereas old granule cells facilitate pattern completion. *Cell* 149, 188–201. doi: 10.1016/j.cell.2012.01.046
- Narayan, R. K., Michel, M. E., Ansell, B., Baethmann, A., Bieganski, A., Bracken, M. B., et al. (2002). Clinical trials in head injury. *J. Neurotrauma* 19, 503–557.
- Neuberger, E. J., Swietek, B., Corrubia, L., Prasanna, A., and Santhakumar, V. (2017). Enhanced dentate neurogenesis after brain injury undermines long-term neurogenic potential and promotes seizure susceptibility. *Stem Cell Rep.* 9, 972–984. doi: 10.1016/j.stemcr.2017.07.015
- Newell, E. A., Todd, B. P., Luo, Z., Evans, L. P., Ferguson, P. J., and Bassuk, A. G. (2019). A mouse model for juvenile, lateral fluid percussion brain injury reveals sex-dependent differences in neuroinflammation and functional recovery. *J. Neurotrauma* 37, 635–646. doi: 10.1089/neu.2019.6675
- Ngwenya, L., and Danzer, S. (2018). Impact of traumatic brain injury on neurogenesis. *Front. Neurosci.* 12:1014. doi: 10.3389/fnins.2018.01014
- Obernier, K., and Alvarez-Buylla, A. (2019). Neural stem cells: origin, heterogeneity and regulation in the adult mammalian brain. *Development* 146:dev156059. doi: 10.1242/dev.156059
- Park, E. H., Burghardt, N. S., Dvorak, D., Hen, R., and Fenton, A. A. (2015). Experience-dependent regulation of dentate gyrus excitability by adult-born granule cells. *J. Neurosci.* 35, 11656–11666. doi: 10.1523/jneurosci.0885-15.2015
- Paterno, R., Metheny, H., and Cohen, A. S. (2018). Memory deficit in an object location task after mild TBI is associated with impaired early object exploration and both are restored by branched chain amino acid dietary therapy. *J. Neurotrauma* 35, 2117–2124. doi: 10.1089/neu.2017.5170
- Paxinos, G., and Franklin, K. B. J. (2019). *Paxinos and Franklin's the Mouse Brain in Stereotaxic Coordinates*. Cambridge, MA: Academic Press.
- Peters, A. J., Villasana, L. E., and Schnell, E. (2018). Ketamine alters hippocampal cell proliferation and improves learning in mice after traumatic brain injury. *Anesthesiology* 129, 278–295. doi: 10.1097/aln.0000000000002197
- Piao, C.-S., Stoica, B. A., Wu, J., Sabirzhanov, B., Zhao, Z., Cabatbat, R., et al. (2013). Late exercise reduces neuroinflammation and cognitive dysfunction after traumatic brain injury. *Neurobiol. Dis.* 54, 252–263. doi: 10.1016/j.nbd.2012.12.017
- Ratliff, W. A., Mervis, R. F., Citron, B. A., Schwartz, B., Rubovitch, V., Schreiber, S., et al. (2020). Effect of mild blast-induced TBI on dendritic architecture of the cortex and hippocampus in the mouse. *Sci. Rep.* 10:2206.
- Report to Congress on Mild Traumatic Brain Injury in the United States (2003). *Report to Congress on Mild Traumatic Brain Injury in the United States*. Available online at: <https://www.cdc.gov/traumaticbraininjury/pdf/mtbireport-a.pdf> (accessed March 21, 2018).
- Riquelme, P. A., Drapeau, E., and Doetsch, F. (2008). Brain micro-ecologies: neural stem cell niches in the adult mammalian brain. *Philos. Trans. R. Soc. Lond. B Biol. Sci.* 363, 123–137. doi: 10.1098/rstb.2006.2016
- Rivera, P. D., Shih, H.-Y., Leblanc, J. A., Cole, M. G., Amaral, W. Z., Mukherjee, S., et al. (2013). Acute and fractionated exposure to high-LET (56)Fe HZE-particle radiation both result in similar long-term deficits in adult hippocampal neurogenesis. *Radiat. Res.* 180, 658–667. doi: 10.1667/rr13480.1
- Rola, R., Mizumatsu, S., Otsuka, S., Morhardt, D. R., Noble-Haeusslein, L. J., Fishman, K., et al. (2006). Alterations in hippocampal neurogenesis following traumatic brain injury in mice. *Exp. Neurol.* 202, 189–199. doi: 10.1016/j.expneurol.2006.05.034
- Sahay, A., Scobie, K. N., Hill, A. S., O'Carroll, C. M., Kheirbek, M. A., Burghardt, N. S., et al. (2011). Increasing adult hippocampal neurogenesis is sufficient to improve pattern separation. *Nature* 472, 466–470. doi: 10.1038/nature09817
- Santhakumar, V., Bender, R., Frotscher, M., Ross, S. T., Hollrigel, G. S., Toth, Z., et al. (2000). Granule cell hyperexcitability in the early post-traumatic rat dentate gyrus: the “irritable mossy cell” hypothesis. *J. Physiol.* 524, 117–134. doi: 10.1111/j.1469-7793.2000.00117.x
- Santhakumar, V., Ratzliff, A. D. H., Jeng, J., Toth, Z., and Soltesz, I. (2001). Long-term hyperexcitability in the hippocampus after experimental head trauma. *Ann. Neurol.* 50, 708–717. doi: 10.1002/ana.1230
- Scharfman, H. E. (2011). *The Dentate Gyrus: A Comprehensive Guide to Structure, Function, and Clinical Implications*. Amsterdam: Elsevier.
- Schurman, L. D., Smith, T. L., Morales, A. J., Lee, N. N., Reeves, T. M., Phillips, L. L., et al. (2017). Investigation of left and right lateral fluid percussion injury in C57BL/6J mice: In vivo functional consequences. *Neurosci. Lett.* 653, 31–38. doi: 10.1016/j.neulet.2017.05.032
- Shapiro, L. A. (2017). Altered hippocampal neurogenesis during the First 7 days after a fluid percussion traumatic brain injury. *Cell Transplant.* 26, 1314–1318. doi: 10.1177/0963689717714099
- Shapiro, L. A., Ribak, C. E., and Jessberger, S. (2008). Structural changes for adult-born dentate granule cells after status epilepticus. *Epilepsia* 49, 13–18. doi: 10.1111/j.1528-1167.2008.01633.x
- Shapiro, L. A., Wang, L., Upadhyaya, P., and Ribak, C. E. (2011). Seizure-induced increased neurogenesis occurs in the dentate gyrus of aged sprague-dawley rats. *Aging Dis.* 2, 286–293.
- Smith, C. J., Johnson, B. N., Elkind, J. A., See, J. M., Xiong, G., and Cohen, A. S. (2012). Investigations on alterations of hippocampal circuit function following mild traumatic brain injury. *J. Vis. Exp.* 69:e4411.
- Smith, C. J., Xiong, G., Elkind, J. A., Putnam, B., and Cohen, A. S. (2015). Brain injury impairs working memory and prefrontal circuit function. *Front. Neurol.* 6:240. doi: 10.3389/fneur.2015.00240
- Sterr, A., Herron, K. A., Hayward, C., and Montaldi, D. (2006). Are mild head injuries as mild as we think? Neurobehavioral concomitants of chronic post-concussion syndrome. *BMC Neurol.* 6:7. doi: 10.1186/1471-2377-6-7
- Sun, D. (2016). Endogenous neurogenic cell response in the mature mammalian brain following traumatic injury. *Exp. Neurol.* 275(Pt 3), 405–410. doi: 10.1016/j.expneurol.2015.04.017
- Sun, D., Daniels, T. E., Rolfe, A., Waters, M., and Hamm, R. (2015). Inhibition of injury-induced cell proliferation in the dentate gyrus of the hippocampus impairs spontaneous cognitive recovery after traumatic brain injury. *J. Neurotrauma* 32, 495–505. doi: 10.1089/neu.2014.3545
- Tanti, A., and Belzung, C. (2013). Neurogenesis along the septo-temporal axis of the hippocampus: are depression and the action of antidepressants region-specific? *Neuroscience* 252, 234–252. doi: 10.1016/j.neuroscience.2013.08.017
- Tanti, A., Rainer, Q., Minier, F., Surget, A., and Belzung, C. (2012). Differential environmental regulation of neurogenesis along the septo-temporal axis of the hippocampus. *Neuropharmacology* 63, 374–384. doi: 10.1016/j.neuropharm.2012.04.022
- Taylor, C. A., Bell, J. M., Breiding, M. J., and Xu, L. (2017). Traumatic brain injury-related emergency department visits, hospitalizations, and deaths - United States, 2007 and 2013. *MMWR Surveill. Summ.* 66, 1–16. doi: 10.15585/mmwr.ss6609a1
- Temprana, S. G., Mongiat, L. A., Yang, S. M., Trincherio, M. F., Alvarez, D. D., Kropff, E., et al. (2015). Delayed coupling to feedback inhibition during a critical period for the integration of adult-born granule cells. *Neuron* 85, 116–130. doi: 10.1016/j.neuron.2014.11.023
- Tensaouti, Y., Yu, T.-S., and Kernie, S. G. (2020). Apolipoprotein E regulates the maturation of injury-induced adult-born hippocampal neurons following traumatic brain injury. *PLoS One* 15:e0229240. doi: 10.1371/journal.pone.0229240
- Tomura, S., Seno, S., Kawachi, S., Miyazaki, H., Sato, S., Kobayashi, Y., et al. (2020). A novel mouse model of mild traumatic brain injury using laser-induced shock waves. *Neurosci. Lett.* 721:134827. doi: 10.1016/j.neulet.2020.134827
- Tran, L. D., Lifshitz, J., Witgen, B. M., Schwarzbach, E., Cohen, A. S., and Grady, M. S. (2006). Response of the contralateral hippocampus to lateral fluid

- percussion brain injury. *J. Neurotrauma* 23, 1330–1342. doi: 10.1089/neu.2006.23.1330
- Tronel, S., Fabre, A., Charrier, V., Oliet, S. H. R., Gage, F. H., and Abrus, D. N. (2010). Spatial learning sculpts the dendritic arbor of adult-born hippocampal neurons. *Proc. Natl. Acad. Sci. U.S.A.* 107, 7963–7968. doi: 10.1073/pnas.0914613107
- van Praag, H., Schinder, A. F., Christie, B. R., Toni, N., Palmer, T. D., and Gage, F. H. (2002). Functional neurogenesis in the adult hippocampus. *Nature* 415, 1030–1034. doi: 10.1038/4151030a
- Villasana, L. E., Kim, K. N., Westbrook, G. L., and Schnell, E. (2015). Functional integration of adult-born hippocampal neurons after traumatic brain injury. *eNeuro* 2:ENEURO.0056-15.2015. doi: 10.1523/ENEURO.0056-15.2015
- Villasana, L. E., Peters, A., McCallum, R., Liu, C., and Schnell, E. (2019). Diazepam inhibits post-traumatic neurogenesis and blocks aberrant dendritic development. *J. Neurotrauma* 36, 2454–2467. doi: 10.1089/neu.2018.6162
- Wang, C.-F., Zhao, C.-C., Liu, W.-L., Huang, X.-J., Deng, Y.-F., Jiang, J., et al. (2019). Depletion of microglia attenuates dendritic spine loss and neuronal apoptosis in the acute stage of moderate traumatic brain injury in mice. *J. Neurotrauma* 37, 43–54. doi: 10.1089/neu.2019.6460
- Wang, X., Gao, X., Michalski, S., Zhao, S., and Chen, J. (2016). Traumatic brain injury severity affects neurogenesis in adult mouse hippocampus. *J. Neurotrauma* 33, 721–733. doi: 10.1089/neu.2015.4097
- Witgen, B. M., Lifshitz, J., Smith, M. L., Schwarzbach, E., Liang, S.-L., Grady, M. S., et al. (2005). Regional hippocampal alteration associated with cognitive deficit following experimental brain injury: a systems, network and cellular evaluation. *Neuroscience* 133, 1–15. doi: 10.1016/j.neuroscience.2005.01.052
- Wood, J. C., Jackson, J. S., Jakubs, K., Chapman, K. Z., Ekdahl, C. T., Kokaia, Z., et al. (2011). Functional integration of new hippocampal neurons following insults to the adult brain is determined by characteristics of pathological environment. *Exp. Neurol.* 229, 484–493. doi: 10.1016/j.expneurol.2011.03.019
- Wu, H., Li, J., Xu, D., Zhang, Q., and Cui, T. (2018). Growth differentiation factor 5 improves neurogenesis and functional recovery in adult mouse hippocampus following traumatic brain injury. *Front. Neurol.* 9:592. doi: 10.3389/fneur.2018.00592
- Wu, M. V., and Hen, R. (2014). Functional dissociation of adult-born neurons along the dorsoventral axis of the dentate gyrus. *Hippocampus* 24, 751–761. doi: 10.1002/hipo.22265
- Wu, M. V., Sahay, A., Duman, R. S., and Hen, R. (2015). Functional differentiation of adult-born neurons along the septotemporal axis of the dentate gyrus. *Cold Spring Harb. Perspect. Biol.* 7:a018978. doi: 10.1101/cshperspect.a018978
- Xiong, Y., Mahmood, A., and Chopp, M. (2013). Animal models of traumatic brain injury. *Nat. Rev. Neurosci.* 14, 128–142.
- Zhang, B.-L., Fan, Y.-S., Wang, J.-W., Zhou, Z.-W., Wu, Y.-G., Yang, M.-C., et al. (2018). Cognitive impairment after traumatic brain injury is associated with reduced long-term depression of excitatory postsynaptic potential in the rat hippocampal dentate gyrus. *Neural Regen. Res.* 13, 1753–1758. doi: 10.4103/1673-5374.238618
- Zhao, C., Deng, W., and Gage, F. H. (2008). Mechanisms and functional implications of adult neurogenesis. *Cell* 132, 645–660. doi: 10.1016/j.cell.2008.01.033
- Zhao, S., Zhou, Y., Gross, J., Miao, P., Qiu, L., Wang, D., et al. (2010). Fluorescent labeling of newborn dentate granule cells in GAD67-GFP transgenic mice: a genetic tool for the study of adult neurogenesis. *PLoS One* 5:e12506. doi: 10.1371/journal.pone.0012506
- Zhou, H., Chen, L., Gao, X., Luo, B., and Chen, J. (2012). Moderate traumatic brain injury triggers rapid necrotic death of immature neurons in the hippocampus. *J. Neuropathol. Exp. Neurol.* 71, 348–359. doi: 10.1097/nen.0b013e31824ea078
- Zhou, Q.-G., Lee, D., Ro, E. J., and Suh, H. (2016). Regional-specific effect of fluoxetine on rapidly dividing progenitors along the dorsoventral axis of the hippocampus. *Sci. Rep.* 6:35572.

Conflict of Interest: The authors declare that the research was conducted in the absence of any commercial or financial relationships that could be construed as a potential conflict of interest.

Copyright © 2021 Clark, Yun, Acquah, Kumar, Metheny, Paixao, Cohen and Eisch. This is an open-access article distributed under the terms of the Creative Commons Attribution License (CC BY). The use, distribution or reproduction in other forums is permitted, provided the original author(s) and the copyright owner(s) are credited and that the original publication in this journal is cited, in accordance with accepted academic practice. No use, distribution or reproduction is permitted which does not comply with these terms.